

# The Interplay of Inverted Redox Potentials and Aromaticity in the Oxidized States of New $\pi$ -Electron Donors: 9-(1,3-Dithiol-2-ylidene)fluorene and 9-(1,3-Dithiol-2-ylidene)thioxanthene Derivatives

Samia Amriou,<sup>[a]</sup> Changsheng Wang,<sup>[a]</sup> Andrei S. Batsanov,<sup>[a]</sup> Martin R. Bryce,\*<sup>[a]</sup> Dmitrii F. Perepichka,<sup>[a, b]</sup> Enrique Ortí,<sup>[c]</sup> Rafael Viruela,<sup>[c]</sup> José Vidal-Gancedo,<sup>[d]</sup> and Concepció Rovira<sup>[d]</sup>

**Abstract:** Derivatives of 9-(1,3-dithiol-2-ylidene)fluorene (**9**) and 9-(1,3-dithiol-2-ylidene)thioxanthene (**10**) have been synthesised using Horner–Wadsworth–Emmons reactions of (1,3-dithiol-2-yl)phosphonate reagents with fluorenone and thioxanthene-9-one. X-ray crystallography, solution electrochemistry, optical spectroscopy, spectroelectrochemistry and simultaneous electrochemistry and electron paramagnetic resonance (SEPR), combined with theoretical calculations performed at the B3P86/6-31G\*\* level, elucidate the interplay of the electronic and structural properties in these mole-

cules. These compounds are strong two-electron donors, and the oxidation potentials depend on the electronic structure of the oxidised state. Two, single-electron oxidations ( $E_1^{\text{ox}} < E_2^{\text{ox}}$ ) were observed for 9-(1,3-dithiol-2-ylidene)fluorene systems (**9**). In contrast, derivatives of 9-(1,3-dithiol-2-ylidene)thioxanthene (**10**) display the unusual phenomenon of inverted potentials ( $E_1^{\text{ox}} > E_2^{\text{ox}}$ ) resulting in a single, two-

electron oxidation process. The latter is due to the aromatic structure of the thioxanthenium cation (formed on the loss of a second electron), which stabilises the dication state ( $\mathbf{10}^{2+}$ ) compared with the radical cation. This contrasts with the nonaromatic structure of the fluorenium cation of system **9**. The two-electron oxidation wave in the thioxanthene derivatives is split into two separate one-electron waves in the corresponding sulfoxide and sulfone derivatives **27–29** owing to destabilisation of the dication state.

**Keywords:** aromaticity • electron donors • fluorene • redox chemistry • thioxanthene

## Introduction

Since the discovery of the remarkable properties of tetrathiafulvalene (TTF, **1**; Scheme 1) and its charge-transfer complexes,<sup>[1]</sup> the 1,3-dithiol-2-ylidene unit has been widely used as a component of new  $\pi$ -electron donor systems due to the high thermodynamic stability of derived cation radical species that contain the heteroaromatic  $6\pi$ -electron dithiolium cation.<sup>[2]</sup> In this context, there has been considerable interest in bis(1,3-dithiole) derivatives with extended  $\pi$ -conjugation between the dithiole rings, notably the incorporation of vinylogous<sup>[3]</sup> and quinoidal<sup>[4–12]</sup> spacer units which reduce intramolecular Coulombic repulsion. For example, the 9,10-bis(1,3-dithiol-2-ylidene)-9,10-dihydroanthracene system (**2**) undergoes a single, quasi-reversible, two-electron oxidation wave to yield a thermodynamically stable dication at  $E^{\text{ox}} \approx -0.03$  V (vs Fc/Fc<sup>+</sup> for R=Me) in cyclic voltammetry (CV) experiments (the oxidation potential varies with the different substituents R).<sup>[5,6,9]</sup> X-ray crystal structures have shown

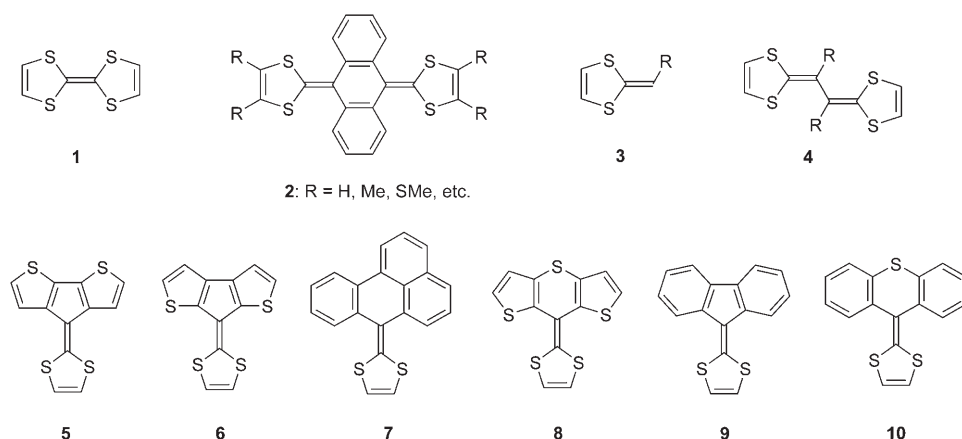
[a] Dr. S. Amriou, Dr. C. Wang, Dr. A. S. Batsanov, Prof. M. R. Bryce, Prof. D. F. Perepichka  
Department of Chemistry, University of Durham  
Durham DH1 3LE (UK)  
Fax: (+44)191-374-4737  
E-mail: m.r.bryce@durham.ac.uk

[b] Prof. D. F. Perepichka  
Chemistry Department, McGill University  
Montreal H3A 2K6 (Canada)

[c] Dr. E. Ortí, Dr. R. Viruela  
Institut de Ciència Molecular, Universitat de València  
46100 Burjassot (Valencia) (Spain)

[d] Dr. J. Vidal-Gancedo, Prof. C. Rovira  
Institut de Ciència de Materials de Barcelona  
C.S.I.C., Campus de la UAB., 08193 Bellaterra (Spain)

Supporting information for this article is available on the WWW under <http://www.chemeurj.org/> or from the author: crystal packing diagrams for compounds **13b** and **18**; crystal structure data for **13b**, **16**, **18**, **28**; cyclic voltammogram of **23**; absorption spectra for compounds **23**, **24** and **18**<sup>2+</sup> in solution.



Scheme 1. TTF (**1**),  $\pi$ -extended TTFs (**2** and **4**) and some related donors containing one dithiole ring.

that a major structural change accompanies oxidation of **2** to the dication: the central anthracenediylidene ring, which is boat shaped in the neutral “butterfly” molecule becomes planar, and a fully aromatic anthracene system with perpendicular,  $6\pi$ -electron 1,3-dithiolium cations is formed.<sup>[4]</sup> Theoretical calculations have established that the steric hindrance introduced by benzoannulation of the central quinodimethane unit determines the saddle shape of the neutral molecules.<sup>[6]</sup> The strong electron-donor ability of this ring system has led to its use as a component of intermolecular<sup>[4,11]</sup> and intramolecular<sup>[7,8,11,12]</sup> charge-transfer systems.

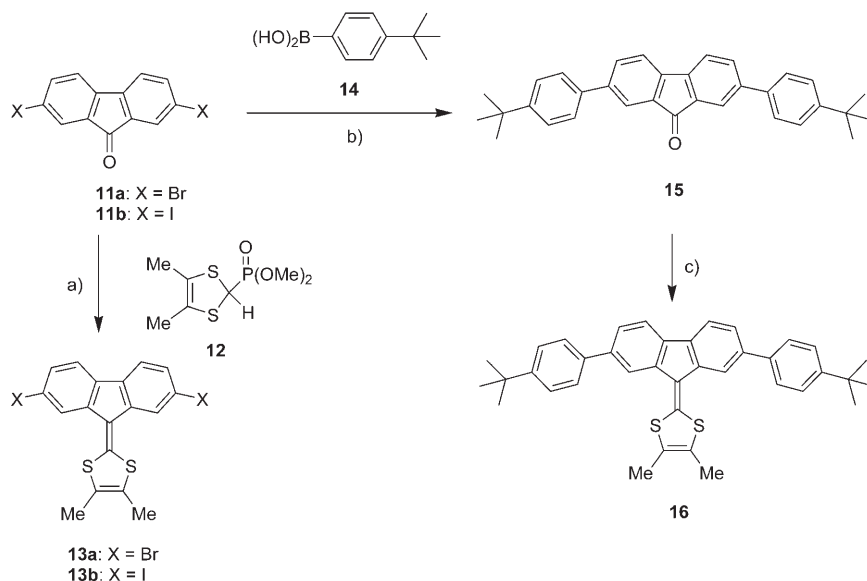
Molecules bearing only one 1,3-dithiol-2-ylidene unit have received much less attention. They are generally weaker electron donors than the bis(1,3-dithiole) systems, but nonetheless they offer a range of interesting redox, spectroscopic and structural properties. For example, compounds of general formula **3**, bearing a hydrogen atom on the exocyclic carbon, readily undergo electrochemical or chemical oxidative dimerisation to afford substituted vinylogous TTFs **4**.<sup>[3d,e]</sup> Other examples are provided by the isomeric cyclopentadithiophene systems **5** and **6**, which adopt planar structures as determined by X-ray analysis and exhibit irreversible oxidation waves at approximately 0.4 V (vs Fc/Fc<sup>+</sup>).<sup>[13]</sup> 7-(1,3-Dithiol-2-ylidene)-7-hydrobenzo-*[d,e]*anthracene (**7**) has also been studied in this context and shown to exhibit multistage redox behaviour in CV experiments with sequential formation of the radical-cation, -dication and -trication species ( $E^{\text{ox}} = +0.15$ ,  $+0.33$  and  $+0.91$  V, respectively, vs Fc/Fc<sup>+</sup> in CH<sub>2</sub>Cl<sub>2</sub>).<sup>[14]</sup> Theoretical cal-

culations show that the neutral molecule **7** and its cation radical exhibit folded butterfly-shaped structures (reminiscent of **2**), whereas the dication comprises a planar polyacenic cation with a perpendicular dithiolium cation. The third oxidation process for **7** corresponds to formation of the dication of the acene unit. Compound **8** undergoes two, single-electron oxidations at low potentials ( $E^{\text{ox}} = -0.07$  and  $+0.06$  V vs Fc/Fc<sup>+</sup>). The neutral form of **8** is nonplanar, whereas the cation radical is planar.<sup>[15]</sup>

Herein we report a detailed study of the synthesis, X-ray crystal structures and electrochemical and spectroscopic characterisation of a range of derivatives of the title systems **9** and **10**, combined with theoretical calculations that shed further light on the interplay of the electronic and structural properties in 1,3-dithiole-derived  $\pi$  donors.

## Results and Discussion

**Synthesis:** The synthesis of 9-(1,3-dithiol-2-ylidene)fluorene derivatives is shown in Scheme 2. 2,7-Dibromo- and 2,7-diiodofluorenone (**11a** and **11b**, respectively) reacted with the carbanion generated from reagent **12** under standard conditions<sup>[5]</sup> to afford the 1,3-dithiol-2-ylidene derivatives **13a** (70% yield) and **13b** (82% yield), respectively. Reaction of



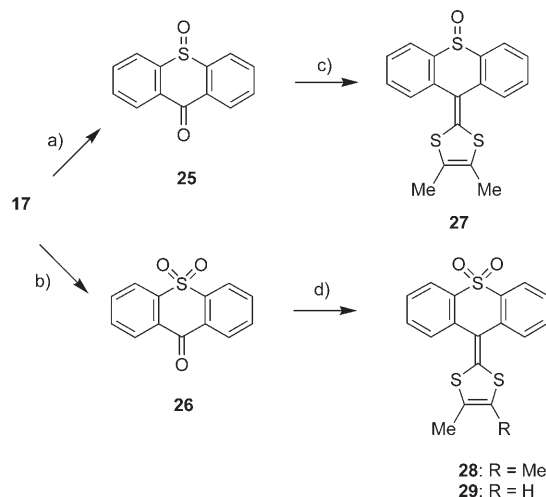
Scheme 2. Reagents and conditions: a) **12**, LDA, THF,  $-78^\circ\text{C}$ , then either **11a**, THF,  $20$ – $50^\circ\text{C}$ , or **11b**, THF,  $20^\circ\text{C}$ ; b) **11a**, DMF, [Pd(PPh<sub>3</sub>)<sub>4</sub>], **14**, Na<sub>2</sub>CO<sub>3</sub> (aq),  $80^\circ\text{C}$ ; c) **12**, LDA, THF,  $78^\circ\text{C}$ , **15**,  $20^\circ\text{C}$ .

**11a** with 4-(*tert*-butyl)phenylboronic acid (**14**) under standard Suzuki conditions using sodium carbonate as base and tetrakis(triphenylphosphino)palladium as catalyst in *N,N*-dimethylformamide (DMF) at 80°C gave compound **15** in 89% yield. Subsequent reaction of **15** with reagent **12**, as described above, gave the expected product **16** in 92% yield. This route to **16** was considerably more efficient than proceeding via **13a** or **13b** for which the analogous Suzuki cross-couplings were less clean and product purification was difficult.

The synthesis of 9-(1,3-dithiol-2-ylidene)thioxanthene derivatives is shown in Scheme 3. Compound **18**<sup>[5]</sup> was obtained in 50% yield from thioxanthene-9-one (**17**) and reagent **12**, analogously to the preparation of **13**. As a precursor to more highly functionalised derivatives of this system, the monomethyl analogue **20** was prepared (48% yield) using reagent **19**.<sup>[10]</sup> Deprotonation of **20** using lithium diisopropylamide (LDA) in THF at -78°C, followed by in situ trapping of the lithiated species with methyl chloroformate gave the methyl ester derivative **21** (67% yield) which was reduced with lithium aluminium hydride to the hydroxymethyl derivative **22** (79% yield). The suitability of compound **22** for further elaboration was established by reaction of its lithium alkoxide salt with 2,5,7-trinitro-4-chlorocarbonylfluoren-9-one<sup>[16]</sup> to afford compound **23** in 20% yield. The electron-acceptor ability of the fluorenone moiety in **23** was increased by conversion to the dicyanomethylene derivative **24** (51% yield) by treatment with malononitrile in DMF. Compounds **23** and **24** assisted in the analysis of the redox properties of the 9-(1,3-dithiol-2-ylidene)thioxanthene system (see below).

The sulfoxide **27** and sulfone derivatives **28** and **29** were synthesised to examine the effect of sulfur oxidation on the redox properties of the system. Thioxanthene-9-one (**17**) was

oxidised to the sulfoxide derivative **25** (14% yield) and the sulfone **26** (81% yield) by using hydrogen peroxide in hexafluoropropan-2-ol<sup>[17]</sup> or acetic acid, respectively (Scheme 4). Subsequent reactions of **25** and **26** with phosphonate ester reagents **12** and **19** gave the products **27–29**.

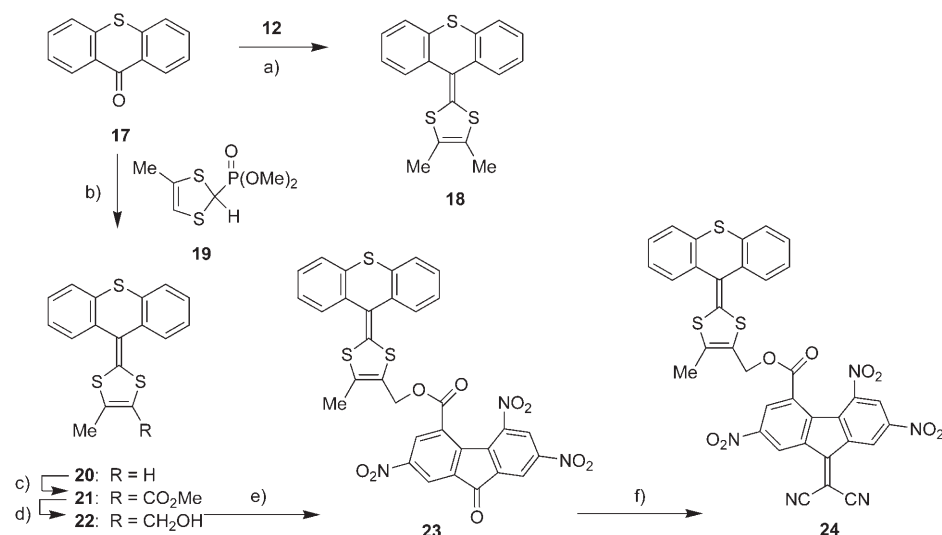


Scheme 4. Reagents and conditions: a)  $\text{H}_2\text{O}_2$  (35% aq), hexafluoro-2-propanol, reflux; b)  $\text{H}_2\text{O}_2$  (35% aq), AcOH, reflux; c) **12**, LDA, THF, -78°C, then **25**, THF, -78→20°C; d) **12** or **19**, LDA, THF, -78°C, then **26**, THF, -78→20°C.

#### Electrochemical, spectroscopic and spectroelectrochemical properties:

The solution electrochemical properties of compounds **13a**, **13b**, **16**, **18**, **20–24** and **27–29** were studied by using cyclic voltammetry (CV) and the data are collated in Table 1, together with literature values for compounds **2** and **5–8** for comparison. Compounds **13a**, **13b** and **16** show two, one-electron oxidation waves, corresponding to the sequential formation of the radical-cation and dication species, with the second wave being irreversible. The additional phenyl rings in **16** lower the oxidation potentials by approximately 100 mV and a third oxidation wave was observed for this compound (Figure 1). The reversibility of the first oxidation process for **13a**, **13b** and **16** is in contrast to the isoelectronic analogues **5** and **6**, although the oxidation potential of all the systems are similar (Table 1).

The (1,3-dithiol-2-ylidene)-thioxanthene derivatives **18** and **20–24** behave very differently.



Scheme 3. Reagents and conditions: a) **12**, LDA, THF, -78°C, then **17**, THF, -78→20°C; b) **19**, LDA, THF, -78°C, then **17**, THF, -78→20°C; c) LDA, THF, -78°C, then  $\text{ClCO}_2\text{Me}$ , -78→20°C; d)  $\text{LiAlH}_4$ , THF, 20°C; e) **22**, *n*BuLi, THF, -100°C, then 2,5,7-trinitro-4-chlorocarbonylfluoren-9-one, -100→20°C; f) malononitrile, DMF, 20°C.

Table 1. Electronic absorption spectra and cyclic voltammetric data.<sup>[a]</sup>

Compound	$\lambda_{\text{max}}$ [nm]	$E_1^{\text{ox}}$ [V] <sup>[b]</sup>	$E_2^{\text{ox}}$ [V]	$E^{\text{red}}$ [V]	Solvent, ref. electrode
<b>2</b> : R = Me <sup>[5]</sup>	433, CH <sub>3</sub> CN	-0.03 (2e)			CH <sub>3</sub> CN, Ag/AgCl
<b>5</b> <sup>[13]</sup>	411, EtOH	+0.45 (ir) <sup>[c]</sup>			EtOH, SCE
<b>6</b> <sup>[13]</sup>	420, CH <sub>2</sub> Cl <sub>2</sub>	+0.4 (ir) <sup>[c]</sup>			CH <sub>2</sub> Cl <sub>2</sub> , SCE
<b>7</b> <sup>[14]</sup>	438, CH <sub>2</sub> Cl <sub>2</sub>	+0.15	+0.33 ( $E_3^{\text{ox}} = 0.91$ )		CH <sub>2</sub> Cl <sub>2</sub> , SCE
<b>8</b> <sup>[15]</sup>	402, CH <sub>2</sub> Cl <sub>2</sub>	-0.07	+0.06		CH <sub>3</sub> CN, SCE
<b>13a</b>	434, CHCl <sub>3</sub>	+0.46	+1.20 <sup>[d]</sup>		CH <sub>2</sub> Cl <sub>2</sub> , Ag/AgNO <sub>3</sub>
<b>13b</b>	437, CHCl <sub>3</sub>	+0.44	+1.11 <sup>[d]</sup>		CH <sub>2</sub> Cl <sub>2</sub> , Ag/AgNO <sub>3</sub>
<b>16</b>	432, CHCl <sub>3</sub>	+0.33	+1.05 <sup>[d]</sup> ( $E_3^{\text{ox}} = 1.25$ <sup>[d]</sup> )		CH <sub>2</sub> Cl <sub>2</sub> , Ag/AgNO <sub>3</sub>
<b>18</b>	384, CHCl <sub>3</sub>	+0.23 (2e)			CH <sub>3</sub> CN, Ag/AgCl
<b>20</b>	379, CHCl <sub>3</sub>	+0.25 (2e)			CH <sub>3</sub> CN, Ag/AgCl
<b>21</b>	368, CHCl <sub>3</sub>	+0.38 (2e)			CH <sub>3</sub> CN, Ag/AgCl
<b>22</b>	376, CHCl <sub>3</sub>	+0.25 (2e)			CH <sub>3</sub> CN, Ag/AgCl
<b>23</b>	600 (br), CHCl <sub>3</sub>	+0.28 (2e)		-0.67, -0.94, -1.70	CH <sub>2</sub> Cl <sub>2</sub> , Ag/AgNO <sub>3</sub>
<b>24</b>	800 (br), CHCl <sub>3</sub>	+0.25 (2e)		-0.36, -0.89, -1.58	CH <sub>2</sub> Cl <sub>2</sub> , Ag/AgNO <sub>3</sub>
<b>27</b>	396, CHCl <sub>3</sub>	+0.56	+0.90 <sup>[d]</sup>		CH <sub>3</sub> CN, Ag/AgCl
<b>28</b>	431, CHCl <sub>3</sub>	+0.58	+1.11 <sup>[d]</sup>		CH <sub>3</sub> CN, Ag/AgCl
<b>29</b>	431, CHCl <sub>3</sub>	+0.59	+1.12		CH <sub>3</sub> CN, Ag/AgCl

[a] See ref. [20] for details of standard procedures and equipment used in these experiments. [b] The potentials were measured versus the Ag/AgCl or Ag/AgNO<sub>3</sub> electrodes and presented versus Fc/Fc<sup>+</sup>, which in our conditions showed +0.45 V versus Ag/AgCl (in CH<sub>3</sub>CN), +0.39 versus SCE (in CH<sub>3</sub>CN), +0.49 V versus Ag/AgCl (in CH<sub>2</sub>Cl<sub>2</sub>), +0.43 versus SCE (in CH<sub>2</sub>Cl<sub>2</sub>), +0.20 V versus Ag/AgNO<sub>3</sub> (in CH<sub>2</sub>Cl<sub>2</sub>). [c] ir = irreversible. [d] The potential of the anodic peak is given for the irreversible oxidation processes.

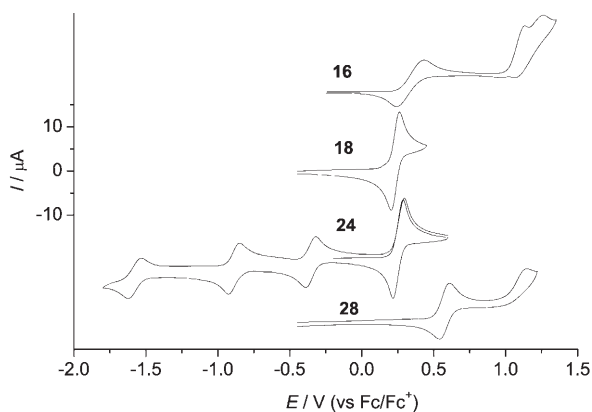


Figure 1. Cyclic voltammetric data for **16**, **18**, **24** and **28**. For details of conditions see Table 1.

A single, two-electron wave is observed in all cases at 0.23–0.38 V (vs Fc/Fc<sup>+</sup>). A general trend in the data, which is consistent with previous observations for derivatives of TTF **1**<sup>[18]</sup> and the quinoidal-TTF **2**,<sup>[10]</sup> is the lowering of the oxidation potential on introducing the electron-donor methyl substituents (by 20 mV, compounds **20**→**18**) and a reverse effect due to the electron-withdrawing carbomethoxy substituent (by 130 mV, **20**→**21**). The oxidation wave for **18** and **20**–**24** is a reversible process with the difference between the potentials of the oxidation peak and the coupled reduction peak  $\Delta E = (E_{\text{pa}}^{\text{ox}} - E_{\text{pc}}^{\text{red}})$  at approximately 40 mV, which is less than the 59 mV value characteristic for a single-electron process, and thus confirms the two-electron oxidation. This low anodic–cathodic peak gap contrasts with the quasi-reversible oxidation of quinoidal-TTF derivatives **2** for which

the corresponding value is approximately 300 mV due to the loss of aromaticity and the large conformational change that occurs on reduction of the dication species **2**<sup>2+</sup> back to the neutral species. The behaviour of **18**, **20** and **21** was essentially unchanged when different electrolytes [tetrabutylammonium (TBA)BF<sub>4</sub>, TBA PF<sub>6</sub>, TBA ClO<sub>4</sub>], scan rates (10–500 mV s<sup>-1</sup>) or lowered temperature (0 °C) were used, whereas a significant increase in the value of  $\Delta E$  was observed in system **2** at lower temperature and higher scan rates.<sup>[6,19]</sup>

The CV data for the donor–acceptor diad compounds **23** and **24** clearly established that the oxidation wave of the (1,3-dithiol-2-ylidene)thioxanthene system involves a two-electron process, as twice the current is

associated with this wave compared with the three, one-electron reductions of the acceptor moieties (Figure 1, and Figure S3 in the Supporting Information). As expected,<sup>[11,20]</sup> the reduction potentials of the fluoren-9-dicyanomethylene unit of **24** are anodically shifted (especially  $E_1^{\text{red}}$ ) compared with that of the fluorenone precursor **23**. The former compound (**24**) is a highly electrochemically amphoteric system, with the difference between the oxidation and reduction potential being only 0.6 V.

We postulated that for the sulfoxide and sulfone derivatives **27**–**29**, in contrast to **18** and **20**–**24**, the radical cation should be observable because the electron-withdrawing effect of SO and SO<sub>2</sub> groups, combined with the lack of aromaticity of an S-oxidised thioxanthemium cation, would make the removal of the second electron more difficult. Indeed, two oxidation waves were observed for **27**–**29** in THF. Coulometric analysis established that the first wave was a one-electron process [0.85e and 0.95e ( $\pm 0.05e$ ) for **27** and **28**, respectively, were deduced from the analysis] leading to the radical cations, **27**<sup>•+</sup> and **28**<sup>•+</sup>, respectively; the second wave (dication formation) was irreversible (Figure 1). It is notable that the first oxidation potentials,  $E_1^{\text{ox}}$ , for both **27**–**29** are very similar (0.56–0.59 V) and are positively shifted relative to the parent system **18**. The second wave,  $E_2^{\text{ox}}$ , however, is 210–220 mV more positive for the sulfone than for the sulfoxide (Table 1) indicating that the second electron is subtracted mostly from the thioxanthemium fragment.

Simultaneous electrochemistry and electron paramagnetic resonance (SEPR) experiments performed in solution for the representative compounds **18** and **29** are in agreement with the CV data. No radical species was detected upon oxi-

dation for compound **18**, which is consistent with the single-stage, 2e process ( $\mathbf{18} \rightarrow \mathbf{18}^{2+}$ ) observed electrochemically. The nondetectable low concentration of  $\mathbf{18}^{++}$  implies a very high disproportionation constant for the radical cation, suggesting reversed values for the oxidation potentials ( $E_2^{\text{ox}} < E_1^{\text{ox}}$ ),<sup>[11,21]</sup> that is, the second electron is removed more easily than the first. Oxidation of **29** gave an intense, very symmetrical EPR signal, with extensive fine structure, assigned to  $\mathbf{29}^{++}$  (Figure 2). Simulation of the spectrum showed that the

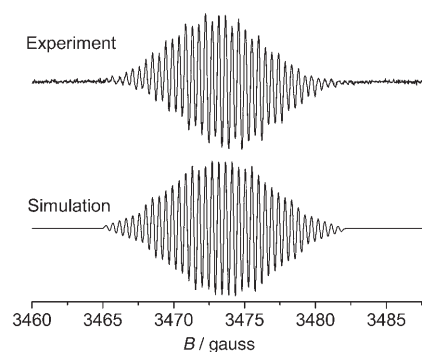


Figure 2. EPR spectrum of in situ electrochemically generated  $\mathbf{29}^{++}$ .

spin is delocalised over the whole molecule. Species  $\mathbf{29}^{++}$  should, therefore, be viewed as a  $\pi$ -extended system. The spin is coupled with the proton and the methyl group of the 1,3-dithiol-2-ylidene moiety and with four sets of two equivalent protons in the aromatic rings showing the following hyperfine coupling constants:  $a_{\text{H}} = 2.24$  G (1H),  $a_{\text{H}} = 1.86$  G (3H),  $a_{\text{H}} = 1.46$  G (2H),  $a_{\text{H}} = 1.38$  G (2H),  $a_{\text{H}} = 1.03$  G (2H),  $a_{\text{H}} = 0.91$  G (2H). The EPR parameters for  $\mathbf{29}^{++}$  ( $g$  factor 2.0059, line width 0.2 G) are very similar to those found for TTF $^{++}$  derivatives.<sup>[22]</sup>

UV-visible absorption spectra reveal a strong absorption from the neutral (1,3-dithiol-2-ylidene)thioxanthene moiety at  $\lambda_{\text{max}} \approx 360$ –385 nm (Table 1). The spectroelectrochemistry

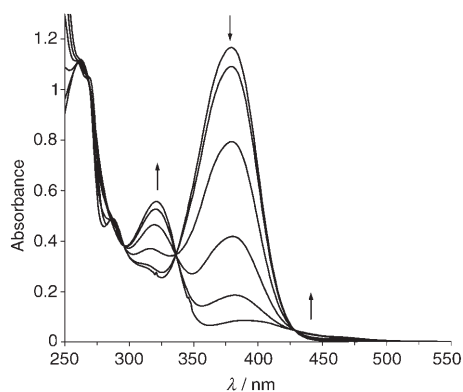


Figure 3. Spectroelectrochemistry of **18**: oxidation process in  $\text{CH}_3\text{CN}$  containing 0.2M TBA $^+$  PF $_6^-$  as electrolyte.

of compound **18** in acetonitrile containing 0.2M TBA $^+$  PF $_6^-$  as electrolyte is shown in Figure 3. Progressive oxidation of the neutral species to the dication was accompanied by a decrease in the peak at  $\lambda_{\text{max}} = 384$  nm and the appearance of two new features at  $\lambda_{\text{max}} = 325$  and  $\approx 400$  nm; the latter being a weaker broad band extending to approximately 500 nm. Upon reversing the potential, the original spectrum of the neutral species was cleanly obtained. The dication salt  $\mathbf{18}^{2+} \cdot (\text{ClO}_4^-)_2$  was isolated by bulk electrolysis (electrolyte TBA $^+$  ClO $_4^-$ ) as a red solid ( $\lambda_{\text{max}} = 325$  and 408 nm in  $\text{CH}_3\text{CN}$ , see Figure S6 in the Supporting Information). This salt was unstable in the presence of air, decomposing to thioxanthene-9-one (**17**). We reported a similar oxidative decomposition of the transient, photolytically generated, cation radical of system **2** to yield the 10-(1,3-dithiol-2-ylidene)anthracene-9(10H)one derivative.<sup>[23]</sup>

The long-wavelength, very weak ( $\epsilon \approx 10 \text{ M}^{-1} \text{ cm}^{-1}$ ) absorption bands observed in the solution UV-visible spectra of diads **23** and **24** were attributed to charge transfer (CT) between the electron-donor dithiolyldene-thioxanthene and the electron-acceptor fluorene moieties. A redshift for the CT transition was observed for **24** (Figure S5 in the Supporting Information;  $\lambda = 700$ –1000 nm) relative to that of **23** ( $\lambda = 500$ –850 nm) owing to the dicyanomethylene group enhancing the electron-acceptor ability. The degree of charge transfer to a dicyanomethylene acceptor unit can be monitored by the lowering of the nitrile stretching frequency in the IR spectrum, compared with that of a neutral 9-dicyanomethylenefluorene analogue.<sup>[20]</sup> For compound **24** this value ( $\tilde{\nu} = 2231 \text{ cm}^{-1}$ ) is very similar to that of neutral nitrofluorene-9-dicyanomethylene derivatives, which suggests that there is very little charge transfer in the ground state. This is in contrast to a related diad system possessing a stronger “extended-TTF” two-electron donor moiety (namely, a derivative of **2**) which has complete charge (electron) transfer ( $\delta_{\text{CT}} \approx 1$ ).<sup>[11]</sup>

**X-ray crystal structures of 13b, 16, 18 and 28:** The single-crystal structures of **13b**, **16**·CDCl $_3$ , **18** and **28**· $\frac{1}{2}$ EtOAc were characterised by means of X-ray diffraction analyses (Figure 4). The dithiole rings are slightly folded along the S $\cdots$ S vector, by 3, 10, 8 and 8°, respectively. The exocyclic C9=C14 bonds are slightly longer [1.369(3), 1.365(5), 1.360(2) and 1.369(2) Å, respectively] than the standard olefinic (R $_2$ C=CR $_2$ ) bond length<sup>[24]</sup> of 1.33(1) Å and are typical for 1,3-dithiol-2-ylidene moieties [average 1.36(1) Å for 115 structures in the November 2004 release of the Cambridge Structural Database].<sup>[25]</sup> Molecule **13b** is nearly planar. In **16** the 1,3-(dithiol-2-ylidene)fluorene system is only slightly puckered, with a 3.8° twist around the C9=C14 bond and a 5.5° angle between benzene rings A and B, although the twists between rings A and C (28°) and between B and D (47°) are substantial. Similar planar conformations have been found in **5**<sup>[13]</sup> and in 4',5'-diazafuorene-1,3-dithiol-2-ylidene ligands coordinated to Ag $^{[26]}$  or Pd.<sup>[27]</sup> By contrast, the thioxanthene system in **18** and **28** adopts a butterfly conformation resembling that of 9,10-bis(1,3-dithiol-2-ylidene)-9,10-dihydroanthracene derivatives **2**:<sup>[4,10,19]</sup> benzene rings A

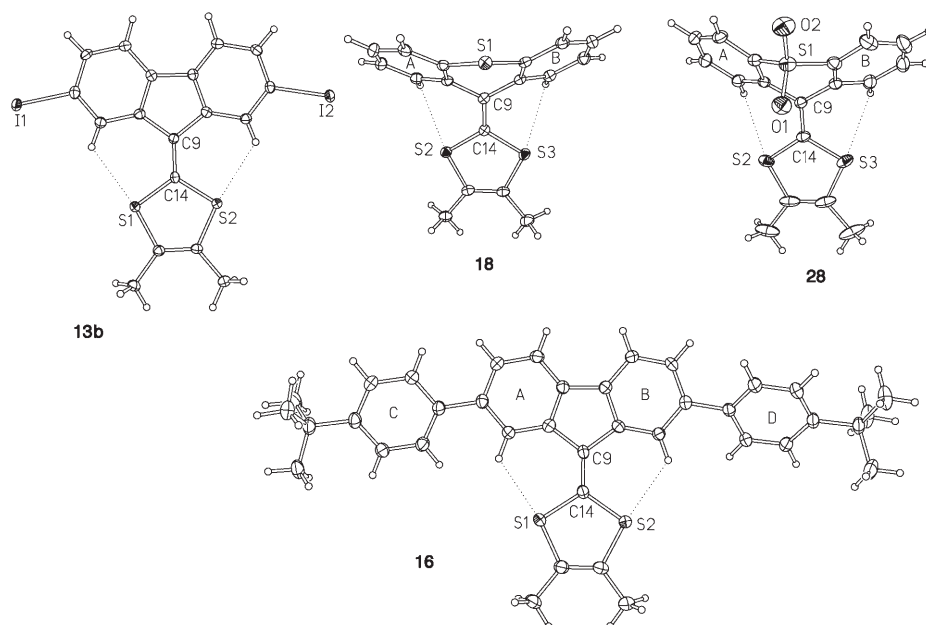


Figure 4. Molecular structures of **13b**, **16**, **18** and **28**, determined by X-ray crystallography, showing thermal ellipsoids at 50% probability.

and B form a dihedral angle of  $145^\circ$  (**18**) and  $138^\circ$  (**28**). In both molecules, the dithiole ring is folded along the S2...S3 vector by  $8^\circ$ , and there is a  $10^\circ$  twist around the C9=C14 bond in **18**.

The warped conformations of **18** and **28** can be explained by steric repulsion between the dithiole S and the *peri* H atoms, which in the imaginary planar structures would be absurdly short (ca.  $2.0 \text{ \AA}$ ). In the experimentally determined structures these distances are increased to  $2.60\text{--}2.68 \text{ \AA}$ , although this is still less than the sum of the van der Waals radii ( $2.91 \text{ \AA}$ ).<sup>[28]</sup> In the fluorene derivatives, the *peri* CH bonds are not parallel to the C9=C14 bond but are directed more outward, thus the S...H distances in the actual, almost planar, structures of **13b** and **16** are increased to  $2.44\text{--}2.49 \text{ \AA}$  (all contacts calculated for the CH distance of  $1.08 \text{ \AA}$ , as determined by neutron diffraction).<sup>[24]</sup> Such distances must still be sterically straining, but the fluorene system (unlike dihydroanthracene or thioxanthene) has no easy way of relieving the strain.

**Theoretical calculations:** To gain a deeper understanding of the experimental data, the molecular structures and electronic properties of compounds **13a**, **16**, **18**, **27** and **28**, in both neutral and oxidised states, were theoretically investigated. Calculations were performed within the density functional theory (DFT) approach at the B3P86/6-31G\*\* level. DFT calculations include electron correlation effects at a relatively low computational cost and are known to provide accurate equilibrium geometries.<sup>[29]</sup>

**Neutral molecules:** The molecular structure of **13a** was optimised under different symmetry restrictions and converged

to a fully planar  $C_{2v}$  structure. The equilibrium geometry calculated is in very good agreement with the X-ray structure obtained for **13b**, the maximum difference between theory and experiment being of only  $0.006 \text{ \AA}$  for the bond lengths. The shortest bond lengths correspond to the carbon-carbon (CC) bond of the dithiole ring ( $1.344 \text{ \AA}$ ) and to the exocyclic C9-C14 bond ( $1.369 \text{ \AA}$ ). The benzene rings of the fluorene unit preserve their aromaticity since all the CC bonds forming these rings have lengths of  $1.40 \pm 0.01 \text{ \AA}$ . The presence of bromine (**13a**) or iodine (**13b**) atoms has no particular effect on the molecular structure. For molecule **16**, calculations predict that the dithiole-fluorene skeleton retains its planarity and that the outer phenyl rings

are twisted by  $37^\circ$ . This rotational angle is intermediate between the X-ray values measured in the crystal ( $28$  and  $47^\circ$ ; Figure 4).

The minimum-energy conformation of **18** corresponds to the butterfly-shaped  $C_s$  structure sketched in Figure 5a. Similar conformations are predicted for compounds **27** and **28**.

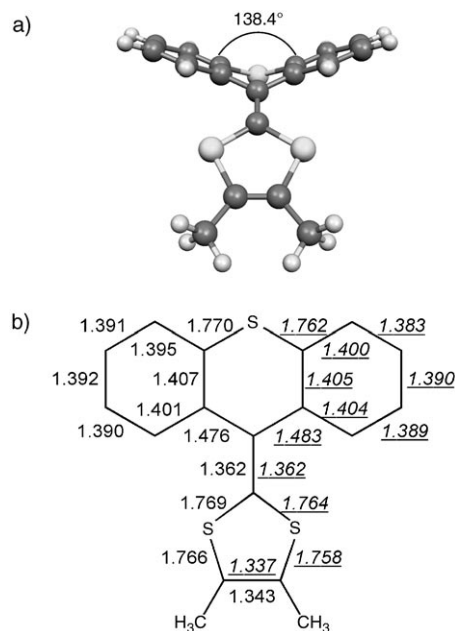


Figure 5. a) Minimum-energy conformation and b) optimised bond lengths (in  $\text{\AA}$ ) calculated at the B3P86/6-31G\*\* level for **18** ( $C_s$  symmetry). Averaged X-ray values of the bond lengths (italics, underlined) are included for comparison.

For **18**, the  $C_s$  structure is computed to be  $21.7 \text{ kcal mol}^{-1}$  more stable than the fully planar  $C_{2v}$  conformation in which short steric contacts ( $2.03 \text{ \AA}$ ) between the dithiole sulfur atoms and the *peri* hydrogen atoms are present. Upon relaxation to the butterfly conformation, the distance between these atoms increases to  $2.70 \text{ \AA}$  (**18**),  $2.73 \text{ \AA}$  (**27**) and  $2.68 \text{ \AA}$  (**28**). As displayed in Figure 5b for **18**, the calculated bond lengths are in very good accord with the averaged X-ray values and show that, as for the dithiole-fluorene derivatives, the two lateral benzene rings retain their aromaticity.

Calculations slightly overestimate the folding of **18** ( $138.4^\circ$ , Figure 5a) compared with X-ray data ( $144.9^\circ$ ) because they are performed for the isolated molecule; in the crystal, there is a tendency to reduce the folding to achieve the most compact packing. Slightly higher foldings are predicted for **28** ( $135.7^\circ$ ), in agreement with the X-ray value ( $138.0^\circ$ ) and especially for **27** ( $130.3^\circ$ ). The sulfoxide oxygen

in **27** actually produces a lengthening effect on the adjacent S–C bonds (**18**:  $1.770 \text{ \AA}$ ; **27**:  $1.801 \text{ \AA}$ ) that is larger than the effect caused by the two sulfone oxygen atoms in **28** ( $1.776 \text{ \AA}$ ). As depicted in Figure 6, the oxygen atom in **27** prefers to be pointing up to the *peri* hydrogen atoms due to the attractive electrostatic interaction with these atoms. This interaction produces a stabilisation of  $5.0 \text{ kcal mol}^{-1}$  with respect to the conformation in which the oxygen atom points down. Calculations also predict the folding of the dithiole rings along the S2...S3 vector (**18**:  $10.6^\circ$ ; **27**:  $8.1^\circ$ ; **28**:  $7.0^\circ$ ).

Figure 7 shows the atomic orbital (AO) composition of the highest-occupied molecular orbital (HOMO) and the lowest-unoccupied molecular orbital (LUMO) of **18**. Similar topologies are found for the fluorene derivatives. Whereas the HOMO is mainly localised on the 1,3-dithiol-2-ylidene unit, the LUMO extends over the carbon skeleton of the thioxanthene or fluorene unit with small contributions from the dithiole ring. Compared to **13a** and **16**, for which the HOMO is calculated at  $-5.83$  and  $-5.62 \text{ eV}$ , the HOMO of **18** lies at  $-5.43 \text{ eV}$ . This destabilisation accounts, in a first

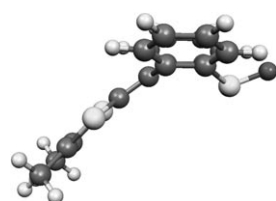


Figure 6. B3P86/6-31G\*\* minimum-energy conformation calculated for **27** ( $C_s$  symmetry).

approach, for the less-positive oxidation potential measured for the thioxanthene derivative (see Table 1).

To investigate the nature of the electronic transitions that give rise to the absorption bands observed in the experimental UV-visible spectra, the electronic excited states of **13a**, **18**, **27** and **28** were calculated by using the time-dependent DFT (TDDFT) approach and the B3P86/6-31G\*\* optimised geometries. Calculations predict that the lowest-energy absorption band observed at  $\lambda = 384 \text{ nm}$  for **18** (Table 1 and Figure 3) is due to the excitation to the first electronic excited state that is calculated at  $3.42 \text{ eV}$  ( $\lambda = 362 \text{ nm}$ ) and corresponds to the promotion of one electron from the HOMO to the LUMO. As shown in Figure 7, the HOMO  $\rightarrow$  LUMO promotion implies some electron-density transfer from the dithiole ring, on which the HOMO is mainly located, to the thioxanthene unit. Calculations therefore suggest that the absorption band implies some intramolecular charge transfer. The absorption band has the same nature for compounds **13a**, **27** and **28**.

**Oxidised compounds:** The equilibrium geometries of the monocations and dication were computed to get a deeper understanding of the oxidation process. As a representative example, Figure 8 displays the minimum-energy conforma-

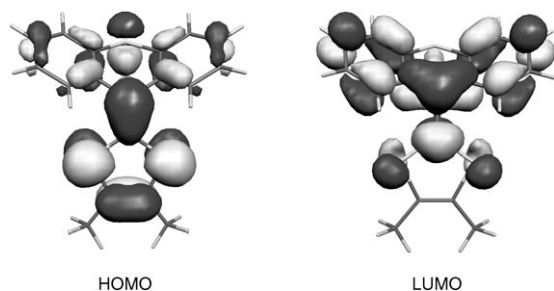


Figure 7. Electron density contours ( $0.03 \text{ e bohr}^{-3}$ ) calculated for the HOMO and the LUMO of **18**.

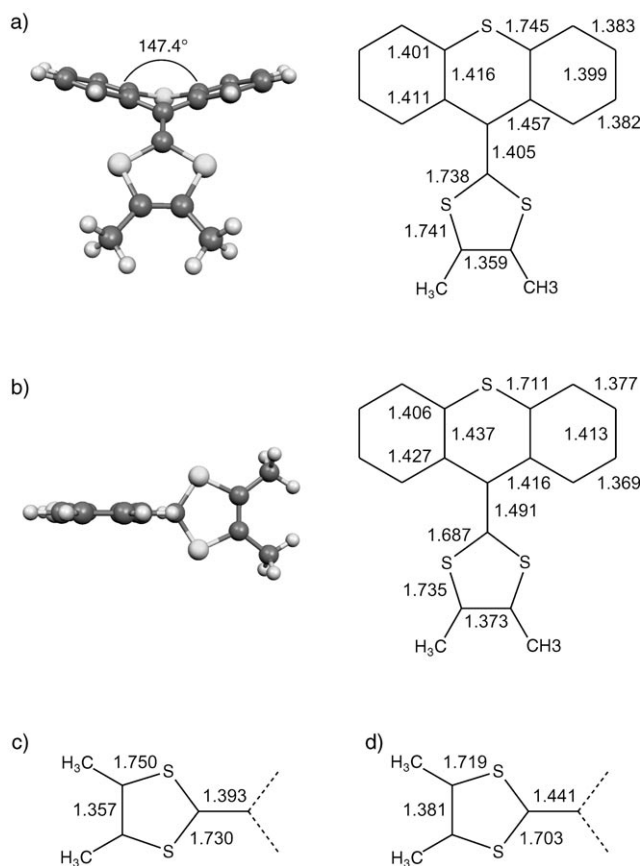


Figure 8. B3P86/6-31G\*\* minimum-energy conformations and optimised bond lengths (in  $\text{\AA}$ ) calculated for a) **18** $^{+\bullet}$  ( $C_s$  symmetry) and b) **18** $^{2+\bullet}$  ( $C_{2v}$  symmetry). B3P86/6-31G\*\*-optimised bond lengths calculated for c) TMTTF $^{+\bullet}$  (planar,  $D_{2h}$  symmetry) and d) TMTTF $^{2+\bullet}$  (planar,  $D_2$  symmetry) are included for comparison.

tions and the optimised bond lengths calculated for  $\mathbf{18}^{+}$  and  $\mathbf{18}^{2+}$ . Oxidation affects the whole molecule by modifying the lengths of the bonds in which the electron density in the HOMO (that is, the orbital from which the electrons are removed) is concentrated. In this way, the largest changes in going to the dication correspond to (compare Figures 5b and 8b) 1) the exocyclic C9–C14 bond, which lengthens from 1.362 Å ( $\mathbf{18}$ ) to 1.491 Å ( $\mathbf{18}^{2+}$ ), 2) the dithiole S–C14 bonds, which shorten from 1.769 to 1.687 Å, 3) the thioxanthene C–S1 bonds, which shorten from 1.770 to 1.711 Å, and 4) the C–C9 bonds, which are reduced from 1.476 to 1.416 Å. Similar changes are found for  $\mathbf{27}$  and  $\mathbf{28}$  (e.g., the C9–C14 bond lengthens from 1.362 to 1.490 Å in  $\mathbf{27}$  and from 1.367 to 1.495 Å in  $\mathbf{28}$ ).

The cation radical of  $\mathbf{18}$  is predicted to retain the butterfly structure of the neutral molecule (see Figure 8a), although is slightly less folded (147.4°). The charge distribution calculated for  $\mathbf{18}^{+}$  using the natural populations analysis (NPA) approach indicates that the charge is extracted from both the dithiole ring, which accumulates a charge of +0.58e, and the thioxanthene unit (+0.42e). The geometry of the dithiolium unit in  $\mathbf{18}^{+}$  is indeed closer to that obtained for the tetramethyl-TTF cation (TMTTF<sup>+</sup>), where both rings bear a charge of +0.5e, than to that found for TMTTF<sup>2+</sup>, where both rings support a charge of +1e (compare Figure 8a, c and d).

The removal of the second electron to form  $\mathbf{18}^{2+}$  leads to more marked effects on the molecular conformation. The lengthening of the exocyclic C9–C14 bond allows rotation of the dithiole ring to minimise the steric interactions of the dithiole sulfur atoms with the *peri* hydrogen atoms. The minimum-energy conformation thus corresponds to the  $C_{2v}$  structure depicted in Figure 8b, in which the dithiole ring lies perpendicular to the fully planar thioxanthene unit. The butterfly  $C_s$  structure obtained for  $\mathbf{18}$  and  $\mathbf{18}^{+}$  was also considered for  $\mathbf{18}^{2+}$ , but it was found to be 9.5 kcal mol<sup>-1</sup> higher in energy. The major structural changes found for the  $\mathbf{18} \rightarrow \mathbf{18}^{2+}$  oxidation process are similar to those reported for  $\mathbf{2}^{[4,6]}$  and  $\mathbf{7}^{[14]}$ . For  $\mathbf{18}^{2+}$ , the dithiole ring and the thioxanthene unit are predicted to support almost identical charges (+0.96e and +1.04e, respectively).

Theoretical results therefore indicate that both the first and the second electrons are extracted from the dithiole and the thioxanthene units of  $\mathbf{18}$ . The  $C_{2v}$  conformation of  $\mathbf{18}^{2+}$  was used as an alternative structure of  $\mathbf{18}^{+}$ , in which an aromatic dithiolium cation (6 $\pi$  electrons) is oriented perpendicularly to the neutral, fully planar thioxanthene radical unit (15 $\pi$  electrons). This structure assumes that the first electron is removed exclusively from the dithiole ring and it was found to be 11.0 kcal mol<sup>-1</sup> higher in energy than the butterfly-shaped  $C_s$  structure. This suggests that  $\mathbf{18}^{+}$  prefers to adopt a charge-delocalised butterfly structure rather than a perpendicular structure with the charge localised on the dithiolium ring. A similar conclusion was reached for the cation radical of  $\mathbf{7}^{[14]}$ .

In contrast to the monocation, the dication  $\mathbf{18}^{2+}$  consists of two singly charged, closed-shell aromatic units (6 $\pi$  and

14 $\pi$  electrons). There is, therefore, a substantial gain in aromaticity on going from  $\mathbf{18}^{+}$  to  $\mathbf{18}^{2+}$ , as is the case with  $\mathbf{2}^{2+}$  (two 6 $\pi$ -electron dithiolium cations and neutral 14 $\pi$ -electron anthracene). This gain of aromaticity accounts for the fact that the first two oxidation processes of  $\mathbf{18}$  coalesce under the same oxidation wave as observed with  $\mathbf{2}$ . The thioxanthonium unit in  $\mathbf{18}^{2+}$  (14 $\pi$  electrons) is more stable than the acenium unit in  $\mathbf{7}^{2+}$  (16 $\pi$  electrons) and, therefore, the extraction of a third electron is not observed for  $\mathbf{18}$ .

The S-oxidised compounds  $\mathbf{27}$  and  $\mathbf{28}$  were calculated to undergo the same structural evolution upon oxidation as compound  $\mathbf{18}$ . However, the presence of the electron-withdrawing SO and SO<sub>2</sub> groups determines that two oxidation waves are observed in the CVs of  $\mathbf{27}$  and  $\mathbf{28}$  instead of the single, two-electron oxidation recorded for  $\mathbf{18}$ . To investigate this effect, compounds  $\mathbf{18}$ ,  $\mathbf{27}$  and  $\mathbf{28}$  were recalculated in solution (CH<sub>3</sub>CN) to take into account solvent effects. The energy required for the first ionisation process (neutral  $\rightarrow$  cation radical) was computed to be slightly higher for  $\mathbf{27}$  (5.59 eV) and  $\mathbf{28}$  (5.73 eV) than for  $\mathbf{18}$  (5.35 eV). This is consistent with the positively shifted  $E_1^{\text{ox}}$  values measured for  $\mathbf{27}$  and  $\mathbf{28}$  (Table 1). In contrast, the energy required for the second ionisation process (cation radical  $\rightarrow$  dication) was found to be significantly larger for  $\mathbf{27}$  (6.62 eV) and  $\mathbf{28}$  (6.84 eV) than for  $\mathbf{18}$  (5.44 eV). This indicates that the removal of the second electron is more difficult for  $\mathbf{27}$  and  $\mathbf{28}$  thus justifying the fact that the two ionisation processes appear as well-separated, one-electron oxidation processes in the CVs of  $\mathbf{27}$  and  $\mathbf{28}$ . These data are consistent with the SEEP results, which showed the spin is delocalised over both moieties.

As found for  $\mathbf{18}$ , electrons are extracted from both the dithiole and the fluorene units in  $\mathbf{13a}$ . For the cation radical, the dithiole ring accumulates a charge of +0.70e. This charge is higher than that obtained for  $\mathbf{18}^{+}$  (+0.58e) showing that electrons are more difficult to remove from the fluorene unit in  $\mathbf{13a}$ . For the dication, both the dithiole ring and the fluorene unit support a charge of +1.00e. As shown in Figure 9 for  $\mathbf{13a}^{2+}$ , the planarity of the fluorene unit is preserved upon oxidation and the dithiole ring twists out of the molecular plane. The exocyclic C9–C14 bond lengthens from 1.370 Å in neutral  $\mathbf{13a}$  to 1.405 Å in  $\mathbf{13a}^{+}$  and 1.444 Å in  $\mathbf{13a}^{2+}$ . This is accompanied by an increase in the twisting angle between the two  $\pi$  systems (14.6° for the cation radical and 38.5° for the dication). The twisting reduces the interaction between the dithiole sulfur atoms and the *peri* hydrogen atoms, which increases in electrostatic character upon oxidation. In the  $\mathbf{13a}^{2+}$  dication, the dithiole sulfur atoms have an NPA net charge of +0.78e and are situated at 2.67 Å from the *peri* hydrogen atoms, which support a charge of +0.28e. In contrast to  $\mathbf{18}^{2+}$ , for which the most stable conformation is fully orthogonal (see Figure 8b), the twisted  $C_2$  structure depicted in Figure 9a for  $\mathbf{13a}^{2+}$  is calculated to be 4.4 kcal mol<sup>-1</sup> lower in energy than the fully perpendicular  $C_{2v}$  structure.

The dication  $\mathbf{13a}^{2+}$  can therefore be visualised as an aromatic dithiolium cation (6 $\pi$  electrons) linked to a fluorenyl

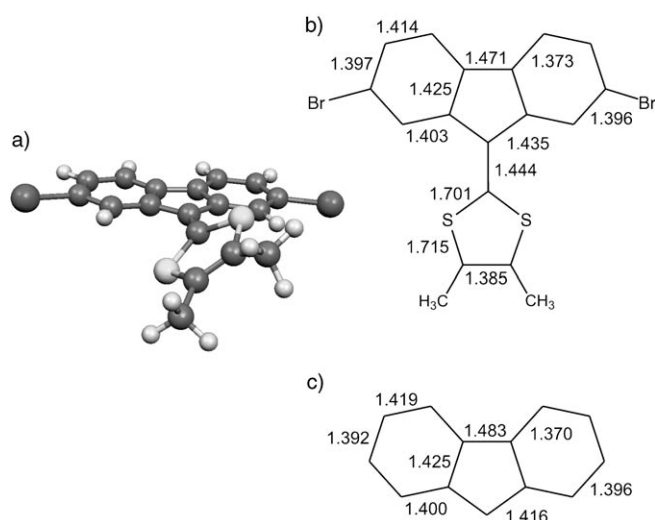


Figure 9. a) Minimum-energy conformation and b) optimised bond lengths (in Å) calculated at the B3P86/6-31G\*\* level for  $\mathbf{13a}^{2+}$  ( $C_2$  symmetry). c) B3P86/6-31G\*\*-optimised bond lengths calculated for the fluorenyl cation.

cation ( $12\pi$  electrons). The structure for the fluorenyl moiety in  $\mathbf{13a}^{2+}$  is very similar to that of the fluorenyl cation (compare Figure 9b and c), and does not show the bond alternation of a typical antiaromatic system, such as the cyclopentadienyl cation ( $0.225$  Å).<sup>[30]</sup> As discussed by Schleyer et al.,<sup>[30]</sup> the term “antiaromatic” is not appropriate for the fluorenyl cation, and these authors prefer the term “nonaromatic”. This could explain the different electrochemical behaviour observed for  $\mathbf{13a}$  when compared with  $\mathbf{18}$ . As discussed above for  $\mathbf{18}$ , a gain in aromaticity is associated with the  $\mathbf{18}^{\cdot+} \rightarrow \mathbf{18}^{2+}$  process (two aromatic units are formed) and the first two oxidation processes coalesce under the same oxidation wave. For  $\mathbf{13a}$ , the aryl unit is not actually aromatised in going to the dication and the two oxidation processes appear well separated in the CV (see Table 1).

As shown in Figure 1, compound  $\mathbf{16}$  presents a third irreversible oxidation process near the solvent limit and separated by only  $0.20$  V from the second oxidation process. Calculations indicate that oxidation in  $\mathbf{16}$  takes place in a different manner than in  $\mathbf{13a}$ . In the cation radical  $\mathbf{16}^{\cdot+}$  the dithiole ring accumulates a charge of  $+0.47e$ , the fluorene unit  $+0.22e$  and the two *tert*-butylphenyl units  $+0.31e$ . In passing to  $\mathbf{16}^{2+}$ , the net charges increase to  $+0.59$ ,  $+0.53$  and  $+0.88e$ , respectively, thus indicating that the phenyl substituents are actively participating in the oxidation process. This result explains the fact that the third oxidation process in  $\mathbf{16}$  ( $\mathbf{16}^{2+} \rightarrow \mathbf{16}^{3+}$ ) takes place at a potential ( $+1.25$  V) similar to that measured for the second oxidation process in  $\mathbf{13a}$  ( $+1.20$  V).

We finally discuss the evolution of the optical properties of  $\mathbf{18}$  upon oxidation. As shown in Figure 3, the intense band observed at  $\lambda = 384$  nm for the neutral system disappears as oxidation takes place and two new features grow up at  $\lambda = 325$  nm and approximately  $400$  nm. TDDFT calcu-

lations for  $\mathbf{18}^{2+}$  assign the low-energy band to the two electronic transitions computed at  $3.14$  eV ( $\lambda = 395$  nm) and  $3.39$  eV ( $\lambda = 366$  nm), which only involve MOs localised on the thioxanthene unit. In contrast, the band at  $\lambda = 325$  nm is due to an electronic transition calculated at  $3.98$  eV ( $\lambda = 311$  nm) which involves the HOMO and the LUMO of the dithiolium cation. The intense band observed at approximately  $\lambda = 260$  nm is again due to an electronic transition ( $4.89$  eV,  $254$  nm) that only concerns the thioxanthene MOs. The electronic spectrum of  $\mathbf{18}^{2+}$  thus results from the addition of the spectroscopic features of the dithiolium and thioxanthenium cations. The electronic interactions between the two  $\pi$  subsystems are limited by the perpendicular disposition they adopt in  $\mathbf{18}^{2+}$ .

## Conclusion

We have prepared two series of novel  $\pi$ -electron donors, 9-(1,3-dithiol-2-ylidene)fluorenes ( $\mathbf{9}$ ) and 9-(1,3-dithiol-2-ylidene)thioxanthenes ( $\mathbf{10}$ ), and studied in detail their electrochemical and spectroscopic properties as well as their molecular and electronic structures (by means of X-ray analysis and DFT calculations, respectively). All these compounds are strong two-electron donors, but the oxidation potentials depend critically on the electronic structure of the oxidised state. Whereas standard two, single-electron oxidations ( $E_1^{\text{ox}} < E_2^{\text{ox}}$ ) were observed for 9-(1,3-dithiol-2-ylidene)fluorene systems, the unusual phenomenon of inverted potentials ( $E_1^{\text{ox}} > E_2^{\text{ox}}$ ) in 9-(1,3-dithiol-2-ylidene)thioxanthene derivatives results in a single, two-electron oxidation process. The latter is due to the aromatic structure of the thioxanthenium cation (formed on the loss of a second electron), which stabilises the dication state compared with the radical cation and contrasts with the nonaromatic structure of the fluorenyl cation. The two-electron oxidation wave in thioxanthene derivatives can be split into two separate one-electron waves by destabilisation of the dication state in S-oxide derivatives. An added attraction of systems  $\mathbf{9}$  and  $\mathbf{10}$  is that they can be readily functionalised to provide new derivatives for inter- and intramolecular charge-transfer studies.

## Experimental Section

**X-ray crystallography:** X-ray diffraction experiments (see Table S1 in the Supporting Information) were carried out on a SMART 3-circle diffractometer with a 1 K CCD area detector, using graphite-monochromated  $\text{MoK}\alpha$  radiation ( $\lambda = 0.71073$  Å) and a Cryostream (Oxford Cryosystems) open-flow  $\text{N}_2$  cryostat. Numerical absorption correction based on real crystal shape was applied for  $\mathbf{13b}$  and  $\mathbf{16}$ . The structures were solved by direct methods and refined by using full-matrix least squares against  $F^2$  of all data with SHELXTL 5.1 software (Bruker AXS, Madison, Wisconsin, U.S.A., 1997). The solvent of crystallisation (deuteriochloroform in  $\mathbf{16}$ ; ethyl acetate in  $\mathbf{28}$ ) is disordered. CCDC-285998 ( $\mathbf{13b}$ ), -285999 ( $\mathbf{16}$ ), -286000 ( $\mathbf{18}$ ) and -286001 ( $\mathbf{28}$ ) contain the supplementary crystallographic data for this paper. These data can be obtained free of charge from the Cambridge Crystallographic Data Centre via [www.ccdc.cam.ac.uk/data\\_request/cif](http://www.ccdc.cam.ac.uk/data_request/cif).

**UV/Vis spectroelectrochemistry:** Spectroelectrochemical data were recorded in CH<sub>3</sub>CN (ca. 10<sup>-4</sup> M solution) with TBA<sup>+</sup>PF<sub>6</sub><sup>-</sup> (0.2 M) as the supporting electrolyte on a Varian Cary 5 spectrophotometer at ambient temperature. Spectra were corrected for background absorption arising from the cell, the electrolyte and the working electrode. The OTTE cell (optical path 1 mm) used a Pt gauze working electrode, Pt wire counter and pseudo-reference electrodes. The solutions were analysed in situ: the working electrode was held at a potential at which no electrochemical work was being done in the cell and the spectrum of the neutral compound was recorded; this was identical to the spectrum recorded for open-circuit conditions. The potential was then increased in 50–200 mV increments and held until equilibrium had been obtained, as evidenced by a sharp drop in the cell current.

**Simultaneous electrochemistry and EPR:** Data were recorded in CH<sub>2</sub>Cl<sub>2</sub> (ca. 10<sup>-4</sup> M solution) with TBA<sup>+</sup>PF<sub>6</sub><sup>-</sup> (0.2 M) as the supporting electrolyte placed in a quartz homemade electrochemical cell equipped with a Pt wire working electrode, Pt wire counter and pseudo-reference electrodes. The cell was placed in the cavity of an X-band Bruker ESP 300E spectrophotometer and spectra were taken after some minutes of electrolysis at a constant potential of 1.04 V.

**Computational details:** All theoretical calculations were carried out with the DFT approach by using the C.02 revision of the Gaussian 03 program package.<sup>[31]</sup> DFT calculations were performed using Becke's three-parameter B3P86 exchange-correlation functional<sup>[32]</sup> and the 6-31G\*\* basis set.<sup>[33]</sup> The B3P86 functional has been recognised as providing equilibrium geometries for sulfur-containing compounds in better accord with experimental data and ab initio post-Hartree-Fock (HF) calculations than the more widely used B3LYP functional.<sup>[34]</sup> The radical cations were treated as open-shell systems and were computed using spin-unrestricted UB3P86 wavefunctions. Vertical electronic excitation energies were determined by means of the TDDFT approach.<sup>[35]</sup> Numerous hitherto reported applications indicate that TDDFT employing current exchange-correlation functionals performs significantly better than HF-based single-excitation theories for the low-lying valence excited states. Net atomic charges were calculated by using the NPA analysis<sup>[36]</sup> included in the natural bond orbital (NBO) algorithm proposed by Weinhold and co-workers.<sup>[37]</sup> Solvent effects were considered with the SCRf (self-consistent-reaction-field) theory using the polarised continuum model (PCM) approach to model the interaction with the solvent.<sup>[38]</sup> The PCM model considers the solvent as a continuous medium with a dielectric constant ( $\epsilon$ ), and represents the solute by means of a cavity built with a number of interlaced spheres.<sup>[39]</sup>

**2,7-Dibromo-9-(4,5-dimethyl-1,3-dithiol-2-ylidene)fluorene (13a):** LDA (5.1 mmol, 2.55 mL of 2 M solution in THF/heptane, ACROS) was added dropwise within 0.5 h to a stirred solution of phosphonate ester **12**<sup>[5]</sup> (1.22 g, 5.1 mmol) in dry THF (30 mL) at -78 °C. A solution of 2,7-dibromofluorenone **11a** (1.70 g, 5.03 mmol) in THF (30 mL, warmed to dissolve) was syringed into the flask through a septum. The cooling bath was removed and the yellow suspension was stirred at 20 °C for 15 h followed by heating to 50 °C for 15 min. Ethanol (50 mL) was added and the solid was collected by suction filtration, then recrystallised from chlorobenzene to yield compound **13a** as yellow needles (1.60 g, 70 %). M.p. 295.0–295.8 °C; <sup>1</sup>H NMR (CDCl<sub>3</sub>, 300 MHz):  $\delta$  = 2.23 (s, 6H), 7.41 (d,  $J$  = 8.1 Hz, 2H), 7.67 (d,  $J$  = 8.0 Hz, 2H), 7.91 ppm (s, 2H); UV/Vis (CHCl<sub>3</sub>):  $\lambda_{\text{max}}$  (log  $\epsilon$ ) = 260 (4.88), 302 (4.21), 315 (4.29), 414 (4.52), 434 nm (4.59); MS (EI):  $m/z$  (%): 452 (100) [ $M^+$ ]; elemental analysis calcd (%) for C<sub>18</sub>H<sub>12</sub>Br<sub>2</sub>S<sub>2</sub>: C 47.81, H 2.67; found: C 47.72, H 2.65.

**2,7-Diiodo-9-(4,5-dimethyl-1,3-dithiol-2-ylidene)fluorene (13b):** 2,7-Diiodofluorenone **11b** (1.81 g, 4.19 mmol) was synthesised in 78 % yield based on the reported method,<sup>[40]</sup> and was added in one portion to a solution of **12** (1.12 g, 4.69 mmol) treated with LDA (4.8 mmol) as above, and the mixture was stirred at 20 °C for 36 h. Product **13b** was obtained as yellow needles after recrystallisation from chlorobenzene (1.88 g, 82 %). M.p.  $\approx$  270 °C (decomp); <sup>1</sup>H NMR (CDCl<sub>3</sub>, 300 MHz):  $\delta$  = 2.23 (s, 6H), 7.56 (d,  $J$  = 8.1 Hz, 2H), 7.61 (dd,  $J_{1,2}$  = 8.0 Hz,  $J_{1,3}$  = 1.2 Hz, 2H), 8.10 ppm (d,  $J_{1,3}$  = 1.2 Hz, 2H); UV/Vis (CHCl<sub>3</sub>):  $\lambda_{\text{max}}$  (log  $\epsilon$ ) = 264 (5.05), 320 (4.58), 417 (4.66), 437 nm (4.73); MS (EI):  $m/z$  (%): 546 (12) [ $M^+$ ], 149 (100); elemental analysis calcd (%) for C<sub>18</sub>H<sub>12</sub>I<sub>2</sub>S<sub>2</sub>: C 39.58, H 2.21;

found: C 39.58, H 2.13. A single crystal suitable for X-ray analysis was obtained by crystallisation from chlorobenzene.

**2,7-Bis[4-(*tert*-butyl)phenyl]fluorenone (15):** [Pd(PPh<sub>3</sub>)<sub>4</sub>] (140 mg) was added to the solution of 2,7-dibromofluorenone (**11a**) (0.676 g, 2 mmol) in degassed DMF (30 mL), and the mixture was stirred at 20 °C for 5 min. 4-(*tert*-Butyl)benzeneboronic acid (0.89 g, 5 mmol) and 1.5 M aqueous sodium carbonate solution (3 mL) were added and the mixture was stirred at 80 °C for 22 h. Water (60 mL) was added to the reaction mixture and the yellow precipitate was collected by suction filtration, washed with water and purified by column chromatography (silica gel, chloroform/hexane 1:1, v/v) to afford **15** as golden yellow crystals (0.79 g, 89 %). M.p. 319.1–319.7 °C; <sup>1</sup>H NMR ([D<sub>2</sub>]tetrachloroethane, 300 MHz):  $\delta$  = 1.40 (s, 9H), 7.51 (d,  $J$  = 8.4 Hz, 2H), 7.60 (d,  $J$  = 7.8, 1H), 7.61 (d,  $J$  = 8.4 Hz, 2H), 7.77 (dd,  $J_{1,2}$  = 7.8 Hz,  $J_{1,3}$  = 1.8 Hz, 1H), 7.92 ppm (d,  $J$  = 1.8 Hz, 1H); <sup>13</sup>C NMR ([D<sub>2</sub>]tetrachloroethane, 75 MHz)  $\delta$  = 197.4, 154.6, 146.3, 145.2, 140.0, 138.6, 136.6, 129.8, 129.5, 126.1, 124.3, 38.1, 34.9 ppm; UV/Vis (CHCl<sub>3</sub>):  $\lambda_{\text{max}}$  (log  $\epsilon$ ) = 294 (5.30), 326 (4.76), 339 (4.68), 446 nm (3.65); MS (EI):  $m/z$  (%): 444 (100) [ $M^+$ ]; elemental analysis calcd (%) for C<sub>33</sub>H<sub>32</sub>O: C 89.15, H 7.25; found: C 88.62, H 7.23.

**2,7-Bis[4-(*tert*-butyl)phenyl]-9-(4,5-dimethyl-1,3-dithiol-2-ylidene)fluorene (16):** Analogous to the synthesis of **13a** and **13b**, compound **12** (0.52 g, 2.18 mmol) was treated with LDA (2.20 mmol) in dry THF (30 mL) at -78 °C. Compound **15** (0.614 g, 1.38 mmol) was added and the mixture was stirred at 20 °C for 24 h. The product was purified on a silica gel column (eluent CS<sub>2</sub>), to afford **16** as bright yellow crystals (0.71 g, 92 %). M.p. > 350 °C; <sup>1</sup>H NMR (CDCl<sub>3</sub> + CS<sub>2</sub>, 300 MHz):  $\delta$  = 1.42 (s, 9H), 2.24 (s, 3H), 7.46 (d,  $J$  = 8.1 Hz, 3H), 7.60 (d, 2H,  $J$  = 8.1 Hz), 7.79 (d,  $J$  = 7.8 Hz, 1H), 7.89 ppm (s, 1H); <sup>13</sup>C NMR (CDCl<sub>3</sub>, 75 MHz):  $\delta$  = 13.1, 31.5, 34.6, 119.7, 121.6, 123.7, 124.2, 125.7, 127.1, 136.4, 138.3, 139.4, 139.9, 150.1 ppm; UV/Vis (CHCl<sub>3</sub>):  $\lambda_{\text{max}}$  (log  $\epsilon$ ) = 273 (4.71), 332 (5.51), 414 (4.31), 432 nm (4.35); MS (EI):  $m/z$  (%): 558 (100) [ $M^+$ ]; elemental analysis calcd (%) for C<sub>38</sub>H<sub>38</sub>S<sub>2</sub>: C 81.67, H 6.85; found: C 81.68, H 6.88. A crystal for X-ray analysis was obtained by slow evaporation of a solution of **16** in a mixture of CDCl<sub>3</sub> and carbon disulfide.

**9-(4,5-Dimethyl-1,3-dithiol-2-ylidene)thioxanthene (18)** was prepared as described previously.<sup>[5]</sup>

**9-(4-Methyl-1,3-dithiol-2-ylidene)thioxanthene (20):** Following the procedure for compound **18**, reagent **19**<sup>[10]</sup> (3.75 g, 16.37 mmol), LDA (12 mL, 18.01 mmol) and **17** (3.47 g, 16.37 mmol) were stirred overnight. Chromatography on silica gel (eluent, dichloromethane/hexane 1:1 v/v) and recrystallisation from ethyl acetate gave compound **20** as yellow crystals (2.45 g, 48 %). M.p. 140–142 °C; <sup>1</sup>H NMR (CDCl<sub>3</sub>):  $\delta$  = 7.65 (t,  $J$  = 7.6 Hz, 2H), 7.40 (dd,  $J$  = 7.6 Hz,  $J$  = 1.2, 2H), 7.28 (t,  $J$  = 7.6 Hz, 2H), 7.19 (t,  $J$  = 7.6 Hz, 2H), 5.79 (d,  $J$  = 1.5 Hz, 1H), 2.0 ppm (d,  $J$  = 1.5 Hz, 3H); <sup>13</sup>C NMR (CDCl<sub>3</sub>):  $\delta$  = 139.1, 137.3, 136.9, 132.23, 132.20, 129.3, 126.95, 126.94, 126.86, 126.83, 126.47, 126.43, 125.9, 121.8, 110.9, 16.0 ppm; MS (EI):  $m/z$  (%): 312 (100) [ $M^+$ ]; UV/Vis (CHCl<sub>3</sub>):  $\lambda_{\text{max}}$  (log  $\epsilon$ ) = 378.8 nm (0.365); elemental analysis calcd (%) for C<sub>17</sub>H<sub>12</sub>S<sub>3</sub>: C 65.34, H 3.87; found: C 65.31, H 3.79.

**9-(4-Methoxycarbonyl-5-methyl-1,3-dithiol-2-ylidene)thioxanthene (21):** LDA (5.64 mL, 8.46 mmol) was added to a stirred solution of compound **20** (2.40 g, 7.69 mmol) in dry THF (50 mL) under N<sub>2</sub> at -78 °C. The reaction mixture was stirred for 2 h. Methyl chloroformate (1.18 mL, 15.38 mmol) was added and the mixture was stirred and left to warm to room temperature overnight. The solvents were removed in vacuo and the residue was purified by chromatography on silica gel with dichloromethane as the eluent; recrystallisation from ethyl acetate gave compound **21** as orange crystals (1.90 g, 67 %). M.p. 206–207 °C; <sup>1</sup>H NMR (CDCl<sub>3</sub>):  $\delta$  = 7.60 (m, 2H), 7.44 (m, 2H), 7.32 (m, 2H), 7.24 (m, 2H), 3.76 (s, 3H), 2.368 ppm (s, 3H); <sup>13</sup>C NMR (CDCl<sub>3</sub>):  $\delta$  = 160.6, 145.4, 136.18, 136.16, 132.44, 132.37, 132.2, 127.23, 127.18, 127.0, 126.9, 126.6, 126.4, 126.1, 126.0, 123.0, 117.0, 52.2, 15.5 ppm; UV/Vis (CHCl<sub>3</sub>):  $\lambda_{\text{max}}$  (log  $\epsilon$ ) = 368.2 nm (0.462); MS (EI):  $m/z$  (%): 370 (100) [ $M^+$ ]; elemental analysis calcd (%) for C<sub>19</sub>H<sub>14</sub>O<sub>2</sub>S<sub>3</sub>: C 61.59, H 3.81; found: C 61.31, H 3.74.

**9-(4-Hydroxymethyl-5-methyl-1,3-dithiol-2-ylidene)thioxanthene (22):** Lithium aluminium hydride (0.61 g, 16.19 mmol) was added to a stirred solution of compound **21** (1.50 g, 4.05 mmol) in dry THF (50 mL) under

$N_2$  at  $-78^\circ\text{C}$ , and the mixture was stirred for 2 h at room temperature. After adding wet sodium sulphate (to quench the unreacted  $\text{LiAlH}_4$ ) dropwise, the reaction was stirred for 30 min. The reaction was filtered through Celite, while washing with methanol. After evaporation of the filtrate, the residue was recrystallised from ethyl acetate to give **22** as yellow crystals (1.09 g, 79%). M.p.  $209\text{--}212^\circ\text{C}$ ;  $^1\text{H NMR}$  ( $[\text{D}_6]\text{DMSO}$ ):  $\delta = 7.57$  (t,  $J = 7.6$  Hz, 2H),  $7.47$  (d,  $J = 7.6$  Hz, 2H),  $7.36$  (m, 2H),  $7.28$  (t,  $J = 7.6$  Hz, 2H),  $5.34$  (t,  $J = 5.6$  Hz, 1H),  $4.17$  (m, 2H),  $1.93$  ppm (s, 3H);  $^{13}\text{C NMR}$  ( $[\text{D}_6]\text{DMSO}$ ):  $136.22, 136.8, 135.9, 131.02, 131.01, 128.0, 127.1, 126.9, 126.8, 126.3, 121.9, 120.6, 56.0, 12.7$  ppm; UV/Vis ( $\text{CHCl}_3$ ):  $\lambda_{\text{max}}$  ( $\log \epsilon$ ) =  $376$  nm (0.314); MS (EI):  $m/z$  (%):  $342$  (100) [ $M^+$ ]; elemental analysis calcd (%) for  $\text{C}_{18}\text{H}_{14}\text{OS}_3$ : C 63.12, H 4.12; found: C 63.07, H 4.20.

**9-[4-(2,5,7-Trinitrofluoren-9-one)carbonyloxymethyl-5-methyl-1,3-dithiol-2-ylidene]thioxanthene (23)**: *n*-Butyllithium (0.91 mL, 1.45 mmol) in THF was added to a stirred solution of compound **22** (0.50 g, 1.45 mmol) in dry THF under  $N_2$  at  $-100^\circ\text{C}$ , and the reaction mixture was stirred for 30 min. Then 2,5,7-trinitro-4-chlorocarbonylfluoren-9-one<sup>[16]</sup> (0.55 g, 1.45 mmol) was added very slowly and the solution was warmed to  $20^\circ\text{C}$  and stirred overnight. After evaporation, the residue was taken up in dichloromethane, and washed several times with water and then dried over magnesium sulfate. The residue was purified by chromatography on silica gel with chloroform as the eluent to afford compound **23** as a black solid (0.20 g, 20%). M.p.  $162\text{--}163^\circ\text{C}$ ;  $^1\text{H NMR}$  ( $\text{CDCl}_3$ ):  $\delta = 8.92$  (s, 1H),  $8.85$  (s, 1H),  $8.79$  (s, 1H),  $8.75$  (s, 1H),  $7.58$  (d,  $J = 7.6$  Hz, 2H),  $7.39$  (t,  $J = 7.6$  Hz, 2H),  $7.28$  (dd,  $J = 7$  m, 2H),  $7.20$  (m, 2H),  $5.06$  (d,  $J = 7$  Hz, 1H),  $5.00$  (d,  $J = 7$  Hz, 1H),  $2.13$  ppm (s, 3H);  $^{13}\text{C NMR}$  ( $\text{CDCl}_3$ ):  $\delta = 184.8, 164.0, 149.6, 149.3, 146.5, 143.4, 139.6, 138.7, 137.7, 136.5, 136.4, 134.0, 132.2, 131.6, 131.4, 130.9, 127.12, 127.09, 126.99, 126.5, 126.4, 126.02, 125.98, 125.3, 122.657, 122.53, 122.0, 118.6, 60.5, 13.6$  ppm; UV/Vis ( $\text{CHCl}_3$ ):  $\lambda_{\text{max}}$  ( $\log \epsilon$ ) =  $361$  nm (0.223); MS (ES):  $m/z$  (%):  $682$  (100) [ $M^+$ ]; elemental analysis calcd (%) for  $\text{C}_{32}\text{H}_{17}\text{N}_3\text{O}_9\text{S}_3$ : C 56.22, H 2.51, N 6.15; found: C 55.95, H 2.55, N 5.89.

**9-[4-(2,5,7-Trinitrofluoren-9-dicyanomethylene)carbonyloxymethyl-1,3-dithiol-2-ylidene]thioxanthene (24)**: Malononitrile (14.5 mg, 0.21 mmol) was added to a stirred solution of compound **23** (0.03 g, 0.043 mmol) dissolved in dry DMF (ca. 2 mL) under  $N_2$  at room temperature, and the solution was stirred overnight at  $20^\circ\text{C}$ . The solvent was removed in vacuo, and methanol was added and the mixture was placed at  $5^\circ\text{C}$  for 30 min. The solid was filtered and washed with methanol to give compound **24** as a green solid (16 mg, 51%). M.p.  $>300^\circ\text{C}$ ;  $^1\text{H NMR}$  ( $\text{CDCl}_3$ ):  $\delta = 9.69$  (d,  $J = 2$  Hz, 1H),  $9.62$  (d,  $J = 2$  Hz, 1H),  $8.98$  (d,  $J = 2$  Hz, 1H),  $8.90$  (d,  $J = 2$  Hz, 1H),  $7.58$  (d,  $J = 7.6$  Hz, 2H),  $7.40$  (d,  $J = 7.6$  Hz, 2H),  $7.15\text{--}7.35$  (m, 4H),  $5.07$  (d,  $J = 7$  Hz, 1H),  $5.00$  (d,  $J = 7$  Hz, 1H),  $2.13$  ppm (s, 3H);  $^{13}\text{C NMR}$  ( $\text{CDCl}_3$ ):  $\delta = 163.9, 153.4, 149.5, 149.0, 147.0, 140.6, 138.9, 137.9, 137.1, 136.8, 136.7, 132.5, 132.2, 131.8, 130.7, 127.4, 127.3, 127.2, 126.8, 126.7, 126.3, 124.9, 124.1, 123.4, 123.0, 118.7, 111.7, 111.6, 60.9, 13.9$  ppm; UV/Vis ( $\text{CHCl}_3$ ):  $\lambda_{\text{max}}$  ( $\log \epsilon$ ) =  $305$  (0.46),  $358$  (0.38),  $374$  nm (0.41); IR (KBr):  $\tilde{\nu} = 2231$  (CN),  $1741$  (CO),  $1636, 1540, 1458, 1344$   $\text{cm}^{-1}$ ; MS (ES):  $m/z$  (%):  $730.4$  (100) [ $M^+$ ]; HRMS: calcd for  $\text{C}_{35}\text{H}_{17}\text{N}_5\text{O}_8\text{S}_3$ :  $731.0239$ ; found:  $731.0225$ .

**Thioxanthene-9-one-S-oxide (25)**: Hydrogen peroxide (35% aqueous solution, 0.32 g, 9.43 mmol) was added to a stirred solution of thioxanthene-9-one **17** (1.0 g, 4.71 mmol) in hexafluoro-2-propanol (5 mL) at  $20^\circ\text{C}$ , and the mixture was refluxed for 15 min. The hydrogen peroxide was quenched by addition of a saturated aqueous solution of sodium sulfite. Then water was added to the mixture; the precipitate was filtered and subjected to chromatography on a silica gel column with hexane/diethyl ether (1:1 v/v) as eluent, to afford compound **25** as yellow crystals (0.146 g, 14%). M.p.  $118\text{--}120^\circ\text{C}$ ;  $^1\text{H NMR}$  ( $\text{CDCl}_3$ ):  $\delta = 8.39$  (dd,  $J = 7.8$  Hz,  $J = 1.2$  Hz, 2H),  $8.19$  (dd,  $J = 7.8$  Hz,  $J = 1.2$  Hz, 2H),  $7.86$  (t,  $J = 7.6$  Hz, 2H),  $7.74$  ppm (t,  $J = 7.6$  Hz, 2H);  $^{13}\text{C NMR}$  ( $\text{CDCl}_3$ ):  $\delta = 180.1, 145.2, 134.0, 131.7, 129.6, 128.8, 127.3$  ppm; UV/Vis ( $\text{CHCl}_3$ ):  $\lambda_{\text{max}}$  ( $\log \epsilon$ ) =  $327$  nm (0.914); MS (EI):  $m/z$  (%):  $228$  (100) [ $M^+$ ]; elemental analysis calcd (%) for  $\text{C}_{13}\text{H}_8\text{O}_2\text{S}$ : C 68.40, H 3.53; found: C 68.25, H 3.50.

**Thioxanthene-9-one-S,S-dioxide (26)**: Hydrogen peroxide (35% aqueous solution, 0.16 g, 4.71 mmol) was added to a stirred solution of thioxanthene-9-one **17** (1.0 g, 4.71 mmol) in acetic acid (20 mL) at  $20^\circ\text{C}$ , and the re-

sulting mixture was put under reflux for 2 h, then cooled to  $20^\circ\text{C}$  to afford a precipitate which was filtered and washed with hexane to afford compound **30** as yellow crystals (0.938 g, 81%). M.p.  $179\text{--}180^\circ\text{C}$ ;  $^1\text{H NMR}$  ( $\text{CDCl}_3$ ):  $\delta = 8.35$  (dd,  $J = 7.5$  Hz,  $J = 1.5$  Hz, 2H),  $8.19$  (dd,  $J = 7.5$  Hz,  $J = 1.5$  Hz, 2H),  $7.88$  (td,  $J = 8$  Hz,  $J = 1.5$  Hz, 2H),  $7.78$  ppm (td,  $J = 8$  Hz,  $J = 1.5$  Hz, 2H);  $^{13}\text{C NMR}$  ( $\text{CDCl}_3$ ):  $\delta = 178.6, 141.2, 134.9, 133.5, 130.9, 129.4, 123.8$  ppm; UV/Vis ( $\text{CHCl}_3$ ):  $\lambda_{\text{max}}$  ( $\log \epsilon$ ) =  $383$  nm (0.253); MS (EI):  $m/z$  (%):  $244$  (53) [ $M^+$ ],  $196$  (100); elemental analysis calcd (%) for  $\text{C}_{13}\text{H}_8\text{O}_3\text{S}$ : C 63.92, H 3.30; found: C 63.69, H 3.29.

**9-(4,5-Dimethyl-1,3-dithiol-2-ylidene)thioxanthene-S-oxide (27)**: Following the procedure for the preparation of **18**, reagent **12** (0.155 g, 0.64 mmol), LDA (0.47 mL, 0.7 mmol) and compound **25** (0.146 g, 0.64 mmol) in THF (40 mL) were stirred overnight. After evaporation and chromatography on silica gel (eluent, dichloromethane), recrystallisation from ethyl acetate gave compound **27** as yellow crystals (0.03 g, 14%). M.p.  $235\text{--}237^\circ\text{C}$ ;  $^1\text{H NMR}$  ( $\text{CDCl}_3$ ):  $\delta = 7.84$  (d,  $J = 8$  Hz, 2H),  $7.73$  (d,  $J = 8$  Hz, 2H),  $7.40$  (m, 4H),  $2.09$  ppm (s, 6H); UV/Vis ( $\text{CHCl}_3$ ):  $\lambda_{\text{max}}$  ( $\log \epsilon$ ) =  $396$  nm (0.209); HRMS:  $m/z$  calcd for  $\text{C}_{18}\text{H}_{14}\text{OS}_3$ :  $342.02067$ ; found:  $342.0217$ .

**9-(4,5-Dimethyl-1,3-dithiol-2-ylidene)thioxanthene-S,S-dioxide (28)**: Directly analogous to the preparation of **27**, compound **26** gave compound **28** as yellow crystals (0.148 g, 10%). M.p.  $243\text{--}244^\circ\text{C}$ ;  $^1\text{H NMR}$  ( $\text{CDCl}_3$ ):  $\delta = 8.06$  (dd,  $J = 8.0$  Hz,  $J = 1.2$  Hz, 2H),  $7.91$  (d,  $J = 8.0$  Hz,  $J = 1.2$  Hz, 2H),  $7.55$  (td,  $J = 8.0$  Hz,  $J = 1.2$  Hz, 2H),  $7.41$  (td,  $J = 8.0$  Hz,  $J = 1.2$  Hz, 2H),  $1.97$  ppm (s, 6H);  $^{13}\text{C NMR}$  ( $\text{CDCl}_3$ ):  $\delta = 144.7, 138.6, 134.9, 132.0, 127.2, 127.1, 123.9, 122.1, 112.8, 13.3$  ppm; UV/Vis ( $\text{CHCl}_3$ ):  $\lambda_{\text{max}}$  ( $\log \epsilon$ ) =  $431$  nm (0.282); MS (EI):  $m/z$  (%):  $358$  (100) [ $M^+$ ]; elemental analysis calcd (%) for  $\text{C}_{18}\text{H}_{14}\text{O}_2\text{S}_3$ : C 60.30, H 3.94; found: C 60.35, H 3.92. A crystal for X-ray analysis was obtained from ethyl acetate.

**9-(4-Methyl-1,3-dithiol-2-ylidene)thioxanthene-S,S-dioxide (29)**: Following the procedure for the preparation of **28**, compound **26** and reagent **19** gave compound **29** as a yellow powder (0.45 g, 49%). M.p.  $184\text{--}186^\circ\text{C}$ ;  $^1\text{H NMR}$  ( $\text{CDCl}_3$ ):  $\delta = 8.06$  (dd,  $J = 8.0$  Hz,  $J = 1.3$  Hz, 2H),  $7.93$  (d,  $J = 8.0$  Hz,  $J = 1.2$  Hz, 2H),  $7.55$  (td,  $J = 8.0$  Hz,  $J = 1.3$  Hz, 2H),  $7.42$  (td,  $J = 8.0$  Hz,  $J = 1.3$  Hz, 2H),  $5.95$  (s, 1H),  $2.10$  ppm (s, 3H);  $^{13}\text{C NMR}$  ( $\text{CDCl}_3$ ):  $\delta = 138.8, 138.3, 134.9, 132.1, 130.7, 127.2, 127.1, 123.9, 113.6, 110.0, 16.5$  ppm; UV/Vis ( $\text{CHCl}_3$ ):  $\lambda_{\text{max}}$  ( $\log \epsilon$ ) =  $431$  nm (0.282); MS (EI):  $m/z$  (%):  $344$  (100) [ $M^+$ ]; elemental analysis calcd (%) for  $\text{C}_{17}\text{H}_{12}\text{O}_2\text{S}_3$ : C 59.27, H 3.51; found: C 59.12, H 3.60.

## Acknowledgements

We thank EPSRC for funding the work in Durham. D.F.P. thanks the Royal Society of Chemistry for a Journals Grant for International Authors for funding a visit to Durham. The work at Valencia was supported by the MEC of Spain and by FEDER funds (Grant BQU2003-05111). Funding from the Generalitat Valenciana (OCYT-GRUPOS03/173) is also acknowledged.

- [1] a) F. Wudl, G. M. Smith, E. Hufnagel, *J. Chem. Soc. D* **1970**, 1453–1454; b) F. Wudl, D. Wobschall, E. J. Hufnagel, *J. Am. Chem. Soc.* **1972**, *94*, 670–672; c) J. Ferraris, D. O. Cowan, V. V. Walatka, J. H. Perlstein, *J. Am. Chem. Soc.* **1973**, *95*, 948–949.
- [2] T. K. Hansen, J. Becher, *Adv. Mater.* **1993**, *5*, 288–292.
- [3] a) T. Sugimoto, H. Awaji, I. Sugimoto, Y. Misaki, T. Kawase, S. Yoneda, Z. Yoshida, *Chem. Mater.* **1989**, *1*, 535–547; b) M. R. Bryce, A. J. Moore, B. K. Tanner, R. Whitehead, W. Clegg, F. Gerson, A. Lamprecht, S. Pfenninger, *Chem. Mater.* **1996**, *8*, 1182–1188; c) Y. Yamashita, M. Tomura, M. B. Zaman, M. Imaeda, *Chem. Commun.* **1998**, 1657–1658; d) P. Hapiot, D. Lorcy, A. Tallec, R. Carlier, A. Robert, *J. Phys. Chem.* **1996**, *100*, 14823–14827; e) A. J. Moore, M. R. Bryce, P. J. Skabara, A. S. Batsanov, L. M. Goldenberg, J. A. K. Howard, *J. Chem. Soc. Perkin Trans. 1* **1997**, 3443–3449; f) P. Frère, P. J. Skabara, *Chem. Soc. Rev.* **2005**, *34*, 69–98.

- [4] M. R. Bryce, A. J. Moore, M. Hasan, G. J. Ashwell, A. T. Fraser, W. Clegg, M. B. Hursthouse, A. I. Karaulov, *Angew. Chem.* **1990**, *102*, 1493–1495; *Angew. Chem. Int. Ed. Engl.* **1990**, *29*, 1450–1452.
- [5] A. J. Moore, M. R. Bryce, *J. Chem. Soc. Perkin Trans. 1* **1991**, 157–168.
- [6] N. Martín, L. Sánchez, C. Seoane, E. Ortí, P. M. Viruela, R. Viruela, *J. Org. Chem.* **1998**, *63*, 1268–1279.
- [7] M. A. Herranz, N. Martín, *Org. Lett.* **1999**, *1*, 2005–2007.
- [8] N. Martín, L. Sánchez, D. M. Guldi, *Chem. Commun.* **2000**, 113–114.
- [9] S.-G. Liu, L. Pérez, N. Martín, L. Echegoyen, *J. Org. Chem.* **2000**, *65*, 9092–9102.
- [10] M. R. Bryce, T. Finn, A. J. Moore, A. S. Batsanov, J. A. K. Howard, *Eur. J. Org. Chem.* **2000**, 51–60.
- [11] D. F. Perepichka, M. R. Bryce, I. F. Perepichka, S. B. Lyubchik, C. A. Christensen, N. Godbert, A. S. Batsanov, E. Levillain, E. J. L. McInnes, J. P. Zhao, *J. Am. Chem. Soc.* **2002**, *124*, 14227–14238.
- [12] B. Insuasti, C. Atienza, C. Seoane, N. Martín, J. Garín, J. Orduna, R. Alcalá, B. Villacampa, *J. Org. Chem.* **2004**, *69*, 6986–6995, and references therein.
- [13] M. Kozaki, S. Tanaka, Y. Yamashita, *J. Org. Chem.* **1994**, *59*, 442–450.
- [14] N. Martín, E. Ortí, L. Sánchez, P. M. Viruela, R. Viruela, *Eur. J. Org. Chem.* **1999**, 1239–1247.
- [15] T. Suzuki, T. Sakimura, S. Tanaka, Y. Yamashita, H. Shiohara, T. Miyashi, *J. Chem. Soc. Chem. Commun.* **1994**, 1431–1432.
- [16] I. F. Perepichka, A. F. Popov, T. V. Orekhova, M. R. Bryce, A. N. Vdovichenko, A. S. Batsanov, L. M. Goldenberg, J. A. K. Howard, N. I. Sokolov, J. L. Megson, *J. Chem. Soc. Perkin Trans. 2* **1996**, 2453–2469.
- [17] K. S. Ravikumar, Y. M. Zhang, J.-P. Begue, D. Bonnet-Delpon, *Eur. J. Org. Chem.* **1998**, 2937–2940.
- [18] A. S. Batsanov, M. R. Bryce, J. N. Heaton, A. J. Moore, P. J. Skabara, J. A. K. Howard, E. Ortí, P. M. Viruela, R. Viruela, *J. Mater. Chem.* **1995**, *5*, 1689–1696.
- [19] M. R. Bryce, M. A. Coffin, M. B. Hursthouse, A. I. Karaulov, K. Müllen, H. Scheich, *Tetrahedron Lett.* **1991**, *32*, 6029–6032.
- [20] D. F. Perepichka, M. R. Bryce, A. S. Batsanov, E. J. L. McInnes, J. P. Zhao, R. D. Farley, *Chem. Eur. J.* **2002**, *8*, 4656–4669.
- [21] H. Kai, D. H. Evans, *J. Electroanal. Chem.* **1997**, *423*, 29–35.
- [22] C. Rovira, J. Veciana, N. Santaló, J. Tarres, J. Cirujeda, E. Molins, J. Llorca, E. Espinosa, *J. Org. Chem.* **1994**, *59*, 3307–3313.
- [23] A. E. Jones, C. A. Christensen, D. F. Perepichka, A. S. Batsanov, A. Beeby, P. J. Low, M. R. Bryce, A. W. Parker, *Chem. Eur. J.* **2001**, *7*, 973–978.
- [24] F. A. Allen, O. Kennard, D. G. Watson, L. Brammer, A. G. Orpen, R. Taylor, *J. Chem. Soc. Perkin Trans. 2* **1987**, S1–S19.
- [25] F. H. Allen, R. Taylor, *Chem. Soc. Rev.* **2004**, *33*, 463–475.
- [26] Q.-Y. Zhu, Y. Zhang, J. Dai, G.-Q. Bian, D.-X. Jia, J.-S. Zhang, L. Guo, *Chem. Lett.* **2003**, *32*, 762–763.
- [27] Q.-Y. Zhu, G.-Q. Bian, J. Dai, D.-X. Jia, Y. Zhang, L. Guo, *Inorg. Chim. Acta* **2003**, *351*, 177–182.
- [28] R. S. Rowland, R. Taylor, *J. Phys. Chem.* **1996**, *100*, 7384–7391.
- [29] W. Koch, M. C. Holthausen, *A Chemist's Guide to Density Functional Theory*, Wiley-VCH, Weinheim, Germany, **2000**.
- [30] For a discussion of aromaticity and antiaromaticity of charged fluorenyl species on the basis of the magnetic susceptibility exaltation parameters, see: a) H. Jiao, P. von R. Schleyer, Y. Mo, M. A. McAllister, T. T. Tidwell, *J. Am. Chem. Soc.* **1997**, *119*, 7075–7083; b) A. D. Allen, T. T. Tidwell, *Chem. Rev.* **2001**, *101*, 1333–1348.
- [31] Gaussian 03, Revision C.02, M. J. Frisch, G. W. Trucks, H. B. Schlegel, G. E. Scuseria, M. A. Robb, J. R. Cheeseman, J. A. Montgomery, Jr., T. Vreven, K. N. Kudin, J. C. Burant, J. M. Millam, S. S. Iyengar, J. Tomasi, V. Barone, B. Mennucci, M. Cossi, G. Scalmani, N. Rega, G. A. Petersson, H. Nakatsuji, M. Hada, M. Ehara, K. Toyota, R. Fukuda, J. Hasegawa, M. Ishida, T. Nakajima, Y. Honda, O. Kitao, H. Nakai, M. Klene, X. Li, J. E. Knox, H. P. Hratchian, J. B. Cross, V. Bakken, C. Adamo, J. Jaramillo, R. Gomperts, R. E. Stratmann, O. Yazyev, A. J. Austin, R. Cammi, C. Pomelli, J. W. Ochterski, P. Y. Ayala, K. Morokuma, G. A. Voth, P. Salvador, J. J. Dannenberg, V. G. Zakrzewski, S. Dapprich, A. D. Daniels, M. C. Strain, O. Farkas, D. K. Malick, A. D. Rabuck, K. Raghavachari, J. B. Foresman, J. V. Ortiz, Q. Cui, A. G. Baboul, S. Clifford, J. Cioslowski, B. B. Stefanov, G. Liu, A. Liashenko, P. Piskorz, I. Komaromi, R. L. Martin, D. J. Fox, T. Keith, M. A. Al-Laham, C. Y. Peng, A. Nanayakkara, M. Challacombe, P. M. W. Gill, B. Johnson, W. Chen, M. W. Wong, C. Gonzalez, J. A. Pople, Gaussian, Inc., Pittsburgh PA, **2003**.
- [32] J. P. Perdew, *Phys. Rev. B* **1986**, *33*, 8822–8824.
- [33] M. M. Francl, W. J. Pietro, W. J. Hehre, J. S. Binkley, M. S. Gordon, D. J. Defrees, J. A. Pople, *J. Chem. Phys.* **1982**, *77*, 3654–3665.
- [34] a) P. M. Viruela, R. Viruela, E. Ortí, J.-L. Brédas, *J. Am. Chem. Soc. Acta A* **1997**, *119*, 1360–1369; b) R. Liu, X. Zhou, H. Kasmai, *Spectrochim. Acta A* **1997**, *53*, 1241–1256; c) J. A. Altmann, N. C. Handy, V. E. Ingamells, *Mol. Phys.* **1997**, *92*, 339–352.
- [35] a) E. Runge, E. K. U. Gross, *Phys. Rev. Lett.* **1984**, *52*, 997–1000; b) E. K. U. Gross, W. Kohn, *Adv. Quantum Chem.* **1990**, *21*, 255; c) E. K. U. Gross, C. A. Ullrich, U. J. Gossmann, *Density Functional Theory* (Eds.: E. K. U. Gross, R. M. Dreizler), Plenum Press, New York, **1995**, p. 149; d) M. E. Casida, *Recent Advances in Density Functional Methods, Part I* (Ed.: D. P. Chong), World Scientific, Singapore, **1995**, p. 155.
- [36] a) A. E. Reed, F. Weinhold, *J. Chem. Phys.* **1983**, *78*, 4066–4073; b) A. E. Reed, R. B. Weinstock, F. Weinhold, *J. Chem. Phys.* **1985**, *83*, 735–746.
- [37] A. E. Reed, L. A. Curtiss, F. Weinhold, *Chem. Rev.* **1988**, *88*, 899–926.
- [38] a) J. Tomasi, M. Persico, *Chem. Rev.* **1994**, *94*, 2027–2094; b) C. S. Cramer, D. G. Truhlar in *Solvent Effects and Chemical Reactivity* (Eds.: O. Tapia, J. Bertrán), Kluwer, Dordrecht, **1996**, p. 1.
- [39] a) S. Miertus, E. Scrocco, J. Tomasi, *Chem. Phys.* **1981**, *55*, 117–119; b) S. Miertus, J. Tomasi, *Chem. Phys.* **1982**, *65*, 239–245; c) M. Cossi, V. Barone, R. Cammi, J. Tomasi, *Chem. Phys. Lett.* **1996**, *255*, 327–335; d) E. Cancès, B. Mennucci, J. Tomasi, *J. Chem. Phys.* **1997**, *107*, 3032–3041; e) V. Barone, M. Cossi, J. Tomasi, *J. Comput. Chem.* **1998**, *19*, 404–417; f) M. Cossi, G. Scalmani, N. Rega, V. Barone, *J. Chem. Phys.* **2002**, *117*, 43–54.
- [40] a) J. Gallos, A. Varvoglis, *J. Chem. Res. Synop.* **1982**, 150–151; b) N. Fukuyama, H. Nishino, K. Kurosawa, *Bull. Chem. Soc. Jpn.* **1987**, *60*, 4363–4368.

Received: October 24, 2005

Published online: February 2, 2006